



Contents lists available at ScienceDirect

Journal of Hydrology

journal homepage: www.elsevier.com/locate/jhydrol

A high resolution coupled hydrologic–hydraulic model (HiResFlood-UCI) for flash flood modeling

Phu Nguyen^{a,d,*}, Andrea Thorstensen^a, Soroosh Sorooshian^a, Kuolin Hsu^a, Amir AghaKouchak^a, Brett Sanders^a, Victor Koren^b, Zhengtao Cui^{b,c}, Michael Smith^b

^a Department of Civil & Environmental Engineering, University of California, Irvine, United States

^b Hydrology Laboratory, National Weather Service, NOAA, United States

^c Lentech Corporation, United States

^d Nong Lam University, Ho Chi Minh City, Viet Nam

ARTICLE INFO

Article history:
Available online xxxxx

Keywords:
Flash flood
HiResFlood-UCI
HL-RDHM
BreZo
Coupled hydrologic–hydraulic model
Distributed model

SUMMARY

HiResFlood-UCI was developed by coupling the NWS's hydrologic model (HL-RDHM) with the hydraulic model (BreZo) for flash flood modeling at decameter resolutions. The coupled model uses HL-RDHM as a rainfall-runoff generator and replaces the routing scheme of HL-RDHM with the 2D hydraulic model (BreZo) in order to predict localized flood depths and velocities. A semi-automated technique of unstructured mesh generation was developed to cluster an adequate density of computational cells along river channels such that numerical errors are negligible compared with other sources of error, while ensuring that computational costs of the hydraulic model are kept to a bare minimum. HiResFlood-UCI was implemented for a watershed (ELDO2) in the DMIP2 experiment domain in Oklahoma. Using synthetic precipitation input, the model was tested for various components including HL-RDHM parameters (*a priori* versus calibrated), channel and floodplain Manning *n* values, DEM resolution (10 m versus 30 m) and computation mesh resolution (10 m+ versus 30 m+). Simulations with calibrated versus *a priori* parameters of HL-RDHM show that HiResFlood-UCI produces reasonable results with the *a priori* parameters from NWS. Sensitivities to hydraulic model resistance parameters, mesh resolution and DEM resolution are also identified, pointing to the importance of model calibration and validation for accurate prediction of localized flood intensities. HiResFlood-UCI performance was examined using 6 measured precipitation events as model input for model calibration and validation of the streamflow at the outlet. The Nash–Sutcliffe Efficiency (NSE) obtained ranges from 0.588 to 0.905. The model was also validated for the flooded map using USGS observed water level at an interior point. The predicted flood stage error is 0.82 m or less, based on a comparison to measured stage. Validation of stage and discharge predictions builds confidence in model predictions of flood extent and localized velocities, which are fundamental to reliable flash flood warning.

© 2015 Elsevier B.V. All rights reserved.

1. Introduction

Flash floods rank highly among natural hazards in terms of the number of people affected and the number of fatalities (Borga et al., 2010), and significant efforts have been made toward understanding flash flood processes as well as modeling and forecasting them (i.e. Gourley et al., 2012; Braud et al., 2014). Hydrologic models for floods have been designed with various levels of complexity from the so-called lumped (e.g. Sacramento Soil Moisture

Accounting – SAC-SMA, Burnash et al., 1973) to semi-lumped (e.g. VIC – Liang et al., 1994) and distributed (e.g. HL-RDHM – Koren et al., 2003, 2004, 2007). Lumped models treat the whole system as one element with single inputs and outputs at a time and do not account for the spatial variability over the domain (Khakbaz et al., 2012). On the other hand, distributed models, which can capture the heterogeneities in the watershed characteristics and hydrometeorological forcings, are suggested to better represent the physical mechanisms of reality. New remote sensing technologies enable distributed data of earth surface characteristics (topography, soil types, land uses) and forcing inputs (precipitation, temperature, evapotranspiration, etc.) for distributed models. Additionally, remote sensing information from the Surface

* Corresponding author at: Dept. of Civil & Environmental Engineering, E/4130 Engineering Gateway, OFFICE: EH 5308, Mail Code: 2175, Irvine, CA 92697, United States. Tel.: +1 949 824 8821.

E-mail address: ndphu@uci.edu (P. Nguyen).

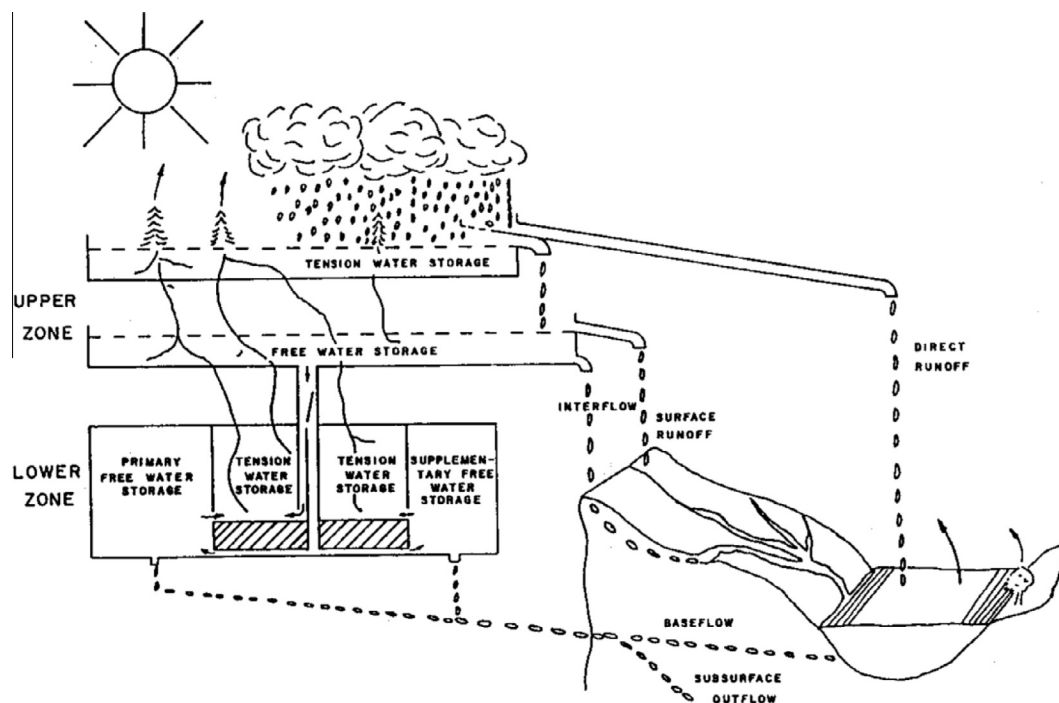


Fig. 1. SAC-SMA rainfall-runoff model conceptualization (from Burnash et al., 1973).

Water and Ocean Topography mission (SWOT, to be launched in 2020) will be useful for distributed calibration/validation (Mersel et al., 2013).

The Office of Hydrologic Development (OHD) at the National Weather Service (NWS) conducted the Distributed Model Inter-comparison Project phases 1&2 (DMIP1&2, Smith et al., 2004, 2012a, 2012b) in the regions of Oklahoma, Arkansas and Missouri. The DMIP experiments were designed to compare the performance of distributed models amongst themselves and to the currently operational lumped model (SAC-SMA) in various aspects of hydrologic modeling such as outlet hydrographs, interior-point hydrographs, model complexity, model calibration, *a priori* parameters and soil moisture. Reed et al. (2004) concluded that in most of the cases of the experiments, lumped models showed better overall performance than distributed models. However, DMIP2 results also suggest that distributed models can account for spatial features of basins and precipitation, and also preserve the water balance in catchments (Smith et al., 2012b).

A hydrologic model (either lumped or distributed) normally involves two main components: a rainfall-runoff estimator and a routing scheme. Water is routed using a routing equation in lumped models or through a cell “conceptual” channel system in distributed models. This can be considered as a weakness of hydrologic models for flood modeling because the “true” physical characteristics of the rivers/channels are not accounted for. Therefore, hydraulic models such as 1D HEC-RAS (US Army Corps of Engineers – USACE), MIKE FLOOD (Danish Hydraulic Institute – DHI), BreZo (Sanders & Begnudelli), and LISFLOOD-FP (University of Bristol) have been applied to simulate floods (Horritt and Bates, 2002; Begnudelli and Sanders, 2006; Bates et al., 2010). One of the main advantages of hydraulic models is that they can simulate flow based on the topography of the channel and floodplain, in accordance with continuity and momentum principles and minimal parameters.

Many efforts have been made to couple hydrologic and hydraulic models for flood modeling purposes. In regional scale, Kim et al. (2012) coupled the Triangulated Irregular Network-Real Time Integrated Basin Simulator (tRIBS) with an Overland Flow Model (OFM) for a watershed of 64 km². Bonnifait et al. (2009) coupled

TOPMODEL with a 1D hydraulic model named CARIMA for reconstructing the catastrophic flood event in the Gard region, France. In large scale, a coupled hydrologic–hydraulic framework of the Interactions between Soil–Biosphere–Atmosphere (ISBA) and LISFLOOD-FP (Bates et al., 2010; Neal et al., 2012) was developed for the Ob River in Siberia (Biancamaria et al., 2009). More recently, Schumann et al. (2013) were successful in coupling the widely used VIC (Liang et al., 1994) with LISFLOOD-FP for forecasting daily flood inundation in large scale for the Lower Zambezi River.

Due to the nature of their design, current coupled hydrologic–hydraulic model systems tend to suffer the inherent trade-off between capturing fine details through the utilization of high resolution and covering extensive geographical domains. A flexible computational mesh makes the proposed coupled system feasible for large areas while maintaining the ability to capture flood details where needed (i.e. closer to the river). The design of the proposed coupling framework itself is unique in that it has the capability to easily switch from uncoupled to coupled mode. In an operational sense, this is extremely valuable as the hydrologic model may be permanently running for an entire large region, such as a river forecast center area, and when more localized area requires detailed simulation of a flash flooding event, the hydraulic component may be activated.

This research aims to develop a high resolution coupled hydrologic–hydraulic model (HiResFlood-UCI) for flash flood modeling. The Hydrology Laboratory Research Distributed Hydrologic Model (HL-RDHM) is coupled with a hydraulic model, BreZo (Sanders & Begnudelli) for flash flood modeling in high resolution at river scale. Further applications of the coupled model are to simulate past severe flash floods, flash flood forecasts and flash flood analysis with various scenarios. HL-RDHM was chosen for the hydrologic component in the HiResFlood-UCI because of its performance in the DMIP series of experiments (e.g., Reed et al., 2004; Smith et al., 2012b, 2013). BreZo has originally been developed for simulating flood extent and flow velocity at river scale and it has been successfully applied for dam breaks (Begnudelli and Sanders, 2006, 2007; Sanders, 2007; Begnudelli et al., 2008).

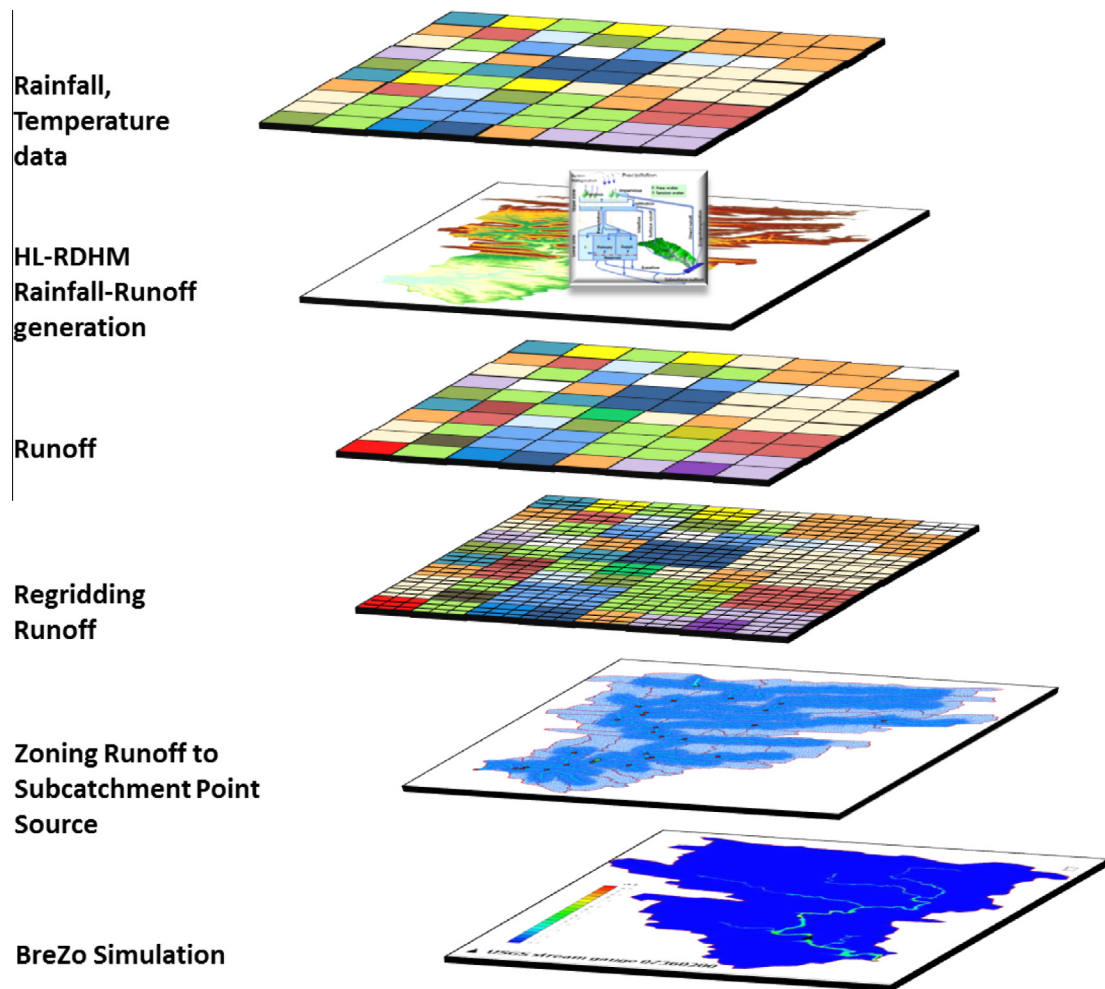


Fig. 2. HiResFlood-UCI coupling framework structure from initial input of rainfall and temperature through HL-RDHM rainfall-runoff generation to the final BreZo simulation output.

2. Description of the coupled model (HiResFlood-UCI)

HiResFlood-UCI is a coupled model based on the heritage of HL-RDHM and BreZo. The coupled model uses HL-RDHM as a rainfall-runoff generator and replaces the routing scheme of HL-RDHM with the 2D hydraulic model (BreZo) for better simulating flash floods at river scale.

2.1. Hydrologic component (HL-RDHM)

The Hydrology Laboratory – Research Distributed Hydrologic Model (HL-RDHM) was developed by the National Weather Service (NWS) Office of Hydrologic Development (OHD), with the basic concepts and structures originated by the Nile Forecast System by [Koren and Barrett \(1995\)](#). HL-RDHM has been developed and implemented for the Contiguous United States (CONUS) for hydrologic research and development. Detailed information can be found in the User Manual V.2.4.2 ([NWS, 2008](#)).

HL-RDHM is a distributed hydrologic model which was designed and implemented for the entire CONUS at a spatial resolution of 1 Hydrologic Rainfall Analysis Project (HRAP) grid (~4 km). HL-RDHM structure can also be applied for any cell resolution and time step length. The model involves three main modules: Snow-17, HL-RDHM, and routing scheme.

The NWS snow accumulation and ablation model (Snow-17) available within HL-RDHM was developed by [Anderson \(1973\)](#). Snow-17 is a conceptual index model for simulating the processes

of snowmelt and snow accumulation based on air temperature. Snow-17 has air temperature and precipitation as model inputs. Snow-17 uses air temperature as the index to determine the energy exchange across the snow-air interface. In distributed application of Snow-17 in HL-RDHM, the depletion curve can be set to a straight line or a snow or no snow relationship for each pixel. More description of the Snow-17 can be found in [Anderson \(1973\)](#), and [NWS \(2008\)](#).

SAC-SMA is the heart of the HL-RDHM model. [Fig. 1](#) represents the SAC-SMA rainfall-runoff model conceptualization. SAC-SMA has two conceptual layers, upper and lower zone storages. Each layer has two basic components, tension water and free water. Tension water is defined as the water that can only be removed from the soil by evaporation or evapotranspiration. The water which can be filled in the voids of the soil and eventually drains out of the soil is considered free water. The upper zone tension water is restricted to the volume of water which can be applied to the dry soil before any component of leakage takes place from the soil. Direct runoff is the fraction of runoff which is due to rainfall over permanent impervious areas of the basin which drains directly to the stream channel. Surface runoff is the fraction of streamflow generated when rainfall exceeds infiltration. Another component of moisture in the unsaturated zone is called the “upper zone free water” which moves laterally through the soil to provide interflow and moves vertically into deeper levels of the soil as percolation. The “lower zone tension water” is the water necessary to fully satisfy moisture requirements based on the molecular

attraction between dry soils and moisture excluding free water in the interstices between the soil molecules. Baseflow is a combination of lateral drainage from lower zone supplementary and primary free water storages. Subsurface outflow is the drainage from lower zone free water storages to aquifers that do not discharge to the stream channel within the basin. More details about SAC-SMA model can be found in [Burnash et al. \(1973\)](#), and [Burnash \(1995\)](#). Forcing data of HL-RDHM include next generation radar (NEXRAD) precipitation data and surface temperature for Snow-17.

The routing scheme has two components: hillslope and channel routing. The hillslope runoff consists of surface (fast) and subsurface (slow) flows. Within a cell, fast runoff is routed over a conceptual uniform hillslope system then combined with the slow flow component and flow from upstream pixels routed through a cell conceptual channel. In the channel routing process, water is moved from upstream to downstream through a topographically based cell-to-cell connectivity sequence. In the routing scheme of HL-RDHM, there are two methods for calculating the relationship between the discharge and cross section area for each cell. *Rutpix7* is based on the channel shape method and *Rutpix9* is based on the rating curve method ([NWS, 2008](#)).

2.2. Hydraulic component (BreZo)

BreZo is a hydraulic model which solves the 2D shallow-water equation using Godunov-type finite volume method ([Toro, 2001](#)) with an unstructured grid of triangular cells. A detailed description of the model can be seen in [Begnudelli and Sanders \(2006\)](#). One of the primary advances of the model is that it was designed for working with an unstructured grid of triangular cells which enables the model to simulate the water flow in varying shapes of the channel/river systems.

2.3. HiResFlood-UCI

A new framework named HiResFlood-UCI has been developed to couple the two models to simulate flash floods. The coupled model is being implemented and tested for some flashy catchments before being applied for the whole CONUS and other parts of the world. In this loose coupling scheme, HL-RDHM and BreZo components are run in parallel. The framework is designed for processing the results from HL-RDHM to the form which BreZo can read as inputs. The whole coupling process follows the steps below and is illustrated in [Fig. 2](#).

2.3.1. Setting up HL-RDHM

HL-RDHM can be executed over the whole CONUS using the *a priori* parameter set provided by NWS to generate surface and subsurface runoffs as input for BreZo. The model can also be set up for a specific domain in the CONUS using calibrated parameter adjustment coefficients provided by NWS.

Hourly rainfall (i.e. Stage IV; PERSIANN – [Hsu et al., 1997](#)) and temperature (i.e. North America Land Data Assimilation Systems – NLDAS) data in coarse resolution (i.e. 4 km) are input to HL-RDHM serving as a rainfall-runoff generator to produce surface and subsurface runoff volumes in the same resolution.

2.3.2. Reprocessing runoffs

The runoff from HL-RDHM in coarse resolution (i.e. 1HRAP ~4 km, 1/2HRAP ~2 km) needs to be regridded into finer resolution (i.e. 10 m). This allows the shape of the subcatchments to be captured in remapping the generated runoff. Each subcatchment has an individual hydrograph of runoff generated by HL-RDHM which is placed on the stream at the point nearest to the centroid of the subcatchment. These hydrographs serve as point sources for BreZo. These multiple point sources are then simultaneously utilized within BreZo to produce flash flood information in appropriate spatial and temporal distributions in the river/channel systems and floodplains.

2.3.3. Procedure to design efficient mesh for BreZo

Mesh resolution plays a highly important role in 2D hydraulic models as it affects both simulation results and computational time. [Hardy et al. \(1999\)](#) concluded that mesh resolution has a greater effect than the friction parameter in the hydraulic simulation in their experiment. [Horritt et al. \(2006\)](#) show that the 2D finite volume model of channel flows in their study is more sensitive to mesh resolution than topographic sampling. There are tools available for designing triangular meshes such as Triangle software ([Shewchuk, 1996](#), available at <http://www.cs.berkeley.edu/~jrs/papers/triangle.pdf>), and Easymesh software, which uses the algorithms developed by [Rebay \(1993\)](#) and [Frey \(1987\)](#).

One of the most important parts of implementation of HiResFlood-UCI is the design of an efficient high resolution triangular mesh. For a catchment, the DEM is downloaded from USGS's National Hydrology Dataset (NHD) at 10 or 30 m resolution. ESRI ArcGIS was employed to process the watershed delineation for subcatchments, subcatchment centroids and stream networks. Using buffering techniques in ArcGIS and the software named Triangle ([Shewchuk, 1996](#)) the mesh can be created with various



Fig. 3. Study area: ELDO2 catchment in DMIP2 experiment.

Table 1

Mesh resolution related to the distance from the river. The mesh has various resolutions ranging from high resolution (i.e. 10 m) along the river where floods often happen, to increasingly coarser (i.e. 30 m, 100 m, 200 m) resolutions as the distance from the river increases.

Buffer zone	Distance from river (m)	Mesh resolution			
		Case 1		Case 2	
		Size (m)	Area (m ²)	Size (m)	Area (m ²)
1	25	10	50	30	450
2	100	30	450	50	1250
3	500	100	5,000	100	5000
4	5000	200	20,000	200	20,000

resolutions ranging from high resolution (i.e. 10 m) along the river where floods often happen, to increasingly coarser (i.e. 30 m, 100 m, 200 m) resolutions as the distance from the river increases. The term of mesh resolution in the model is the length of a leg in a right isosceles triangle that has the equivalent area to the average triangle in the mesh refinement (which may or may not be right isosceles in shape). Depending on the user's particular application, the thickness of the buffer zones around the river network may be adjusted to capture more or less detail as needed. This is especially relevant for main channel width considerations. For example, this mesh development has been applied for the Cedar River watershed in Iowa (mainstream width approximately 200 m) where buffer size (each side of the stream) of the finest mesh was 100 m, and a 25 m size was used for the finest mesh buffer for the Upper Little Missouri River watershed (mainstream width approximately

50 m). The Triangle algorithm refines the triangular mesh based on an area constraint. The computational cost for modeling depends on the number of elements N_E in the domain and the number of time steps N_T as follows,

$$C \sim kN_EN_T \quad (1)$$

where C is the computational cost, k is a factor depending on the numerical scheme (Kim et al., 2014). The proposed mesh design method allows for modeling the whole basin with a minimized number of elements while areas that are important during a flash flood still have the mesh in high resolution. In comparison with a uniform mesh, which has the same resolution as the highest resolution in the proposed method, the computational cost can be reduced as follows,

$$\frac{C_P}{C_U} = \frac{N_{E-U}}{N_{E-P}} \quad (2)$$

where C_P , C_U , N_{E-P} , and N_{E-U} are the computational costs and numbers of elements of the mesh designed by the proposed method and the uniform resolution mesh respectively.

The elevation of each node of the triangular element is interpolated from the DEM using ArcGIS Interpolation Tools. The boundary conditions are assigned to the domain during the mesh creation using Triangle.

2.3.4. BreZo simulation and output processing

BreZo is set up with initial conditions (water level or depth, flow velocity) and boundary conditions (free, wall, inflow and outflow). Initial flow conditions in the channels and over floodplains in BreZo can be assigned as uniform conditions (i.e. dry condition), set to the observed data (water level or depth, flow velocity) or

Table 2

Scenario description: testing HiResFlood-UCI with manning n values (Runs 1–6), HL-RDHM a priori parameters (Run 7), DEM 30 m resolution (Run 8) and mesh 30 m+ resolution (Run 9, Case 2 in Table 1).

Scenario	Manning value – channel	Manning value – floodplain	HL-RDHM parameter	DEM resolution	Mesh resolution
Baseline	0.0925	0.0975	Calibrated	10 m	Case 1 (10 m+)
Run 1	0.0350	0.0350	Calibrated	10 m	Case 1 (10 m+)
Run 2	0.0638	0.0663	Calibrated	10 m	Case 1 (10 m+)
Run 3	0.1213	0.1288	Calibrated	10 m	Case 1 (10 m+)
Run 4	0.0350	0.1600	Calibrated	10 m	Case 1 (10 m+)
Run 5	0.1500	0.0350	Calibrated	10 m	Case 1 (10 m+)
Run 6	0.1500	0.1600	Calibrated	10 m	Case 1 (10 m+)
Run 7	0.0925	0.0975	a priori	10 m	Case 1 (10 m+)
Run 8	0.0925	0.0975	Calibrated	30 m	Case 1 (10 m+)
Run 9	0.0925	0.0975	Calibrated	10 m	Case 2 (30 m+)

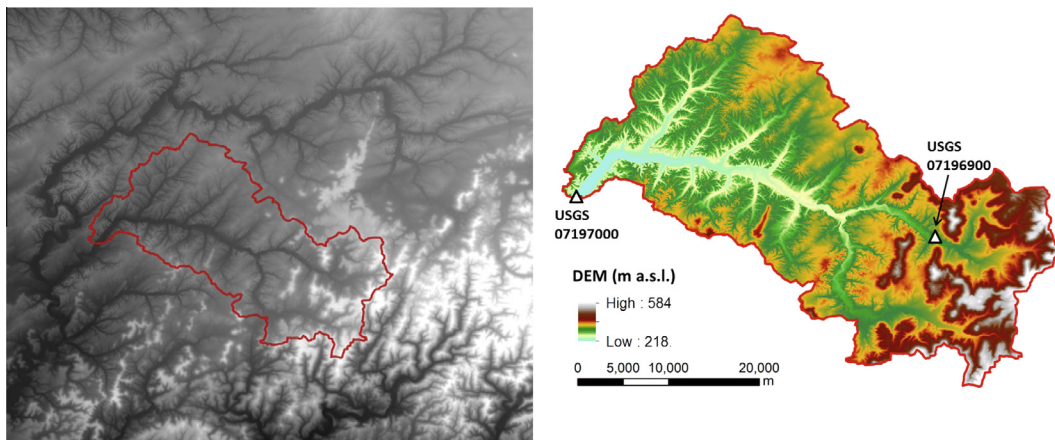


Fig. 4. 10 m DEM of ELD02 extracted from USGS NHD database.

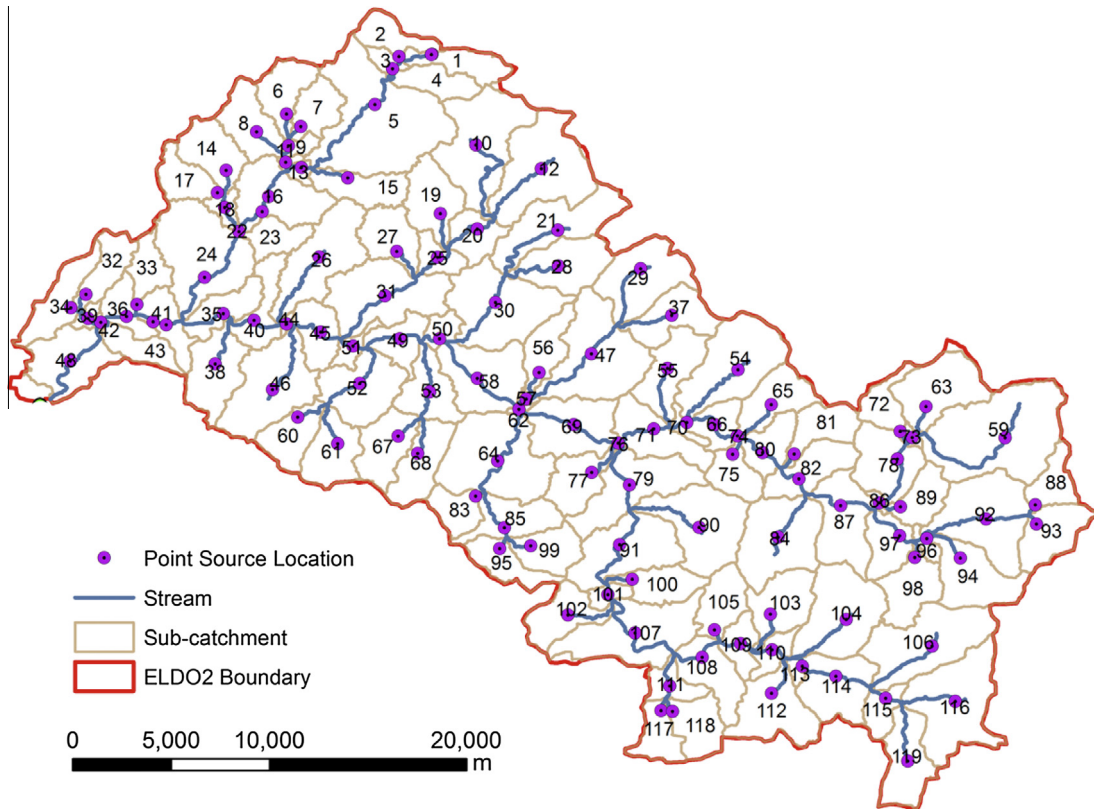


Fig. 5. Subcatchments, stream network and point sources of ELDO2 derived from 10 m DEM using ESRI ArcGIS tools.

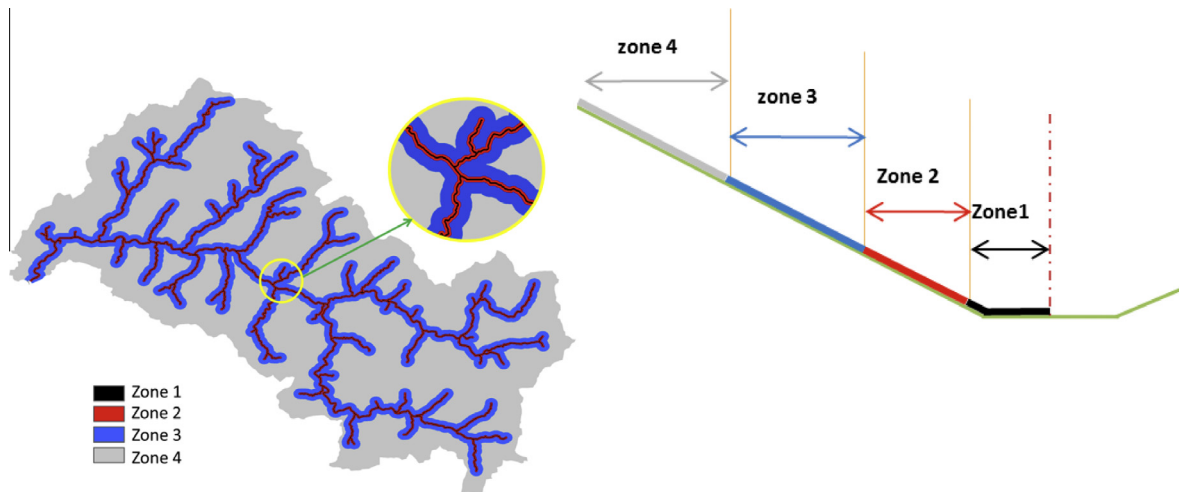


Fig. 6. Mesh design of ELDO2 catchment for BreZo: 4 zones with resolutions progressively increasing toward the rivers (Table 1).

taken as the conditions from a warm-up period. The final option was utilized in this study. BreZo reads the subwatershed runoff hydrographs as pointsource input. The time step for the model run is assigned to a value which allows the global maximum Courant number $Cr \leq 1$ for model stability.

The cross-sections are set at the points of interest to produce discharges. Flooded-area maps and flow velocity maps can be output into Tecplot (visualization software, <http://www.tecplot.com/>) or ArcGIS format. ArcGIS Interpolation Tools can be used to process the flooded maps and flow velocity maps from triangular mesh into regular grid for spatial evaluation or comparison.

2.3.5. Model calibration

HL-RDHM and BreZo in the coupled HiResFlood-UCI can be calibrated separately. HL-RDHM is available with an *a priori* parameter set for the CONUS. The procedure of calibration for HL-RDHM is described in detail in the HL-RDHM User's Manual (NWS, 2008). BreZo is manually calibrated by tuning the Manning *n* roughness values to best fit the hydrograph at the catchment outlet. For areas where there are no stream gauge observation data, an *a priori* parameter set is used for HL-RDHM and Manning *n* roughness values are chosen from Chow's look-up table (Chow, 1959) based on the catchment characteristics.

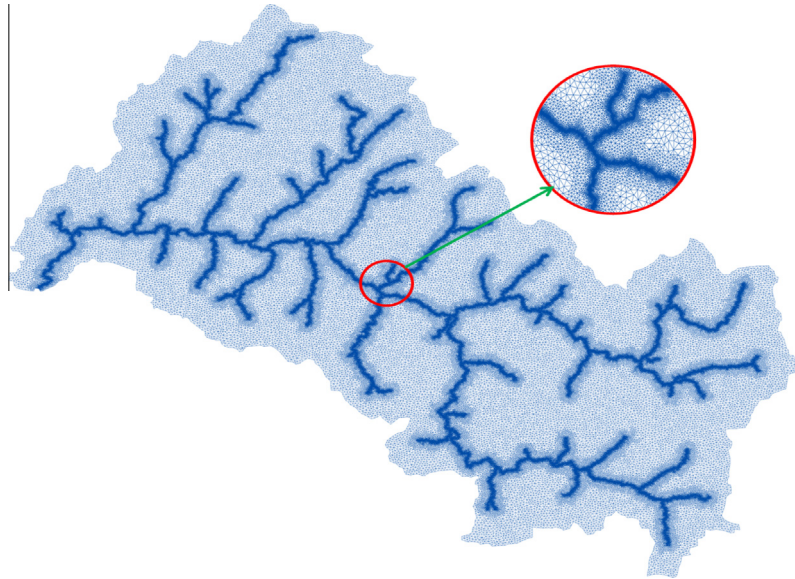


Fig. 7. Example of final unstructured triangular cell mesh of ELD02 for BreZo (Case 1 in Table 1) generated using ArcGIS interpolation tools and the Triangle software.

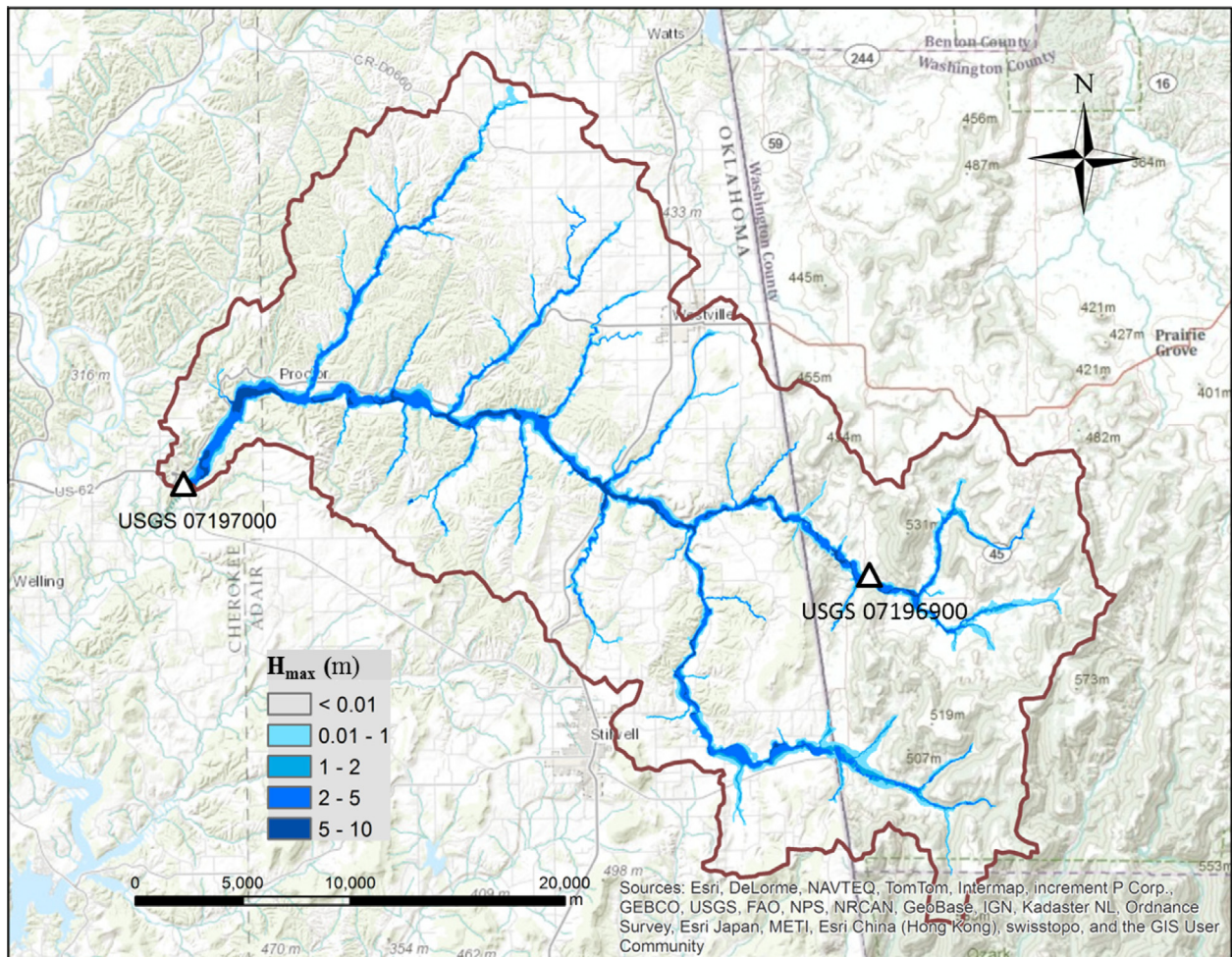


Fig. 8. Flooded map in baseline scenario (see specifications of baseline scenario in Table 2), forced with synthetic precipitation. H_{\max} (m) is the maximum water depth in the simulation.

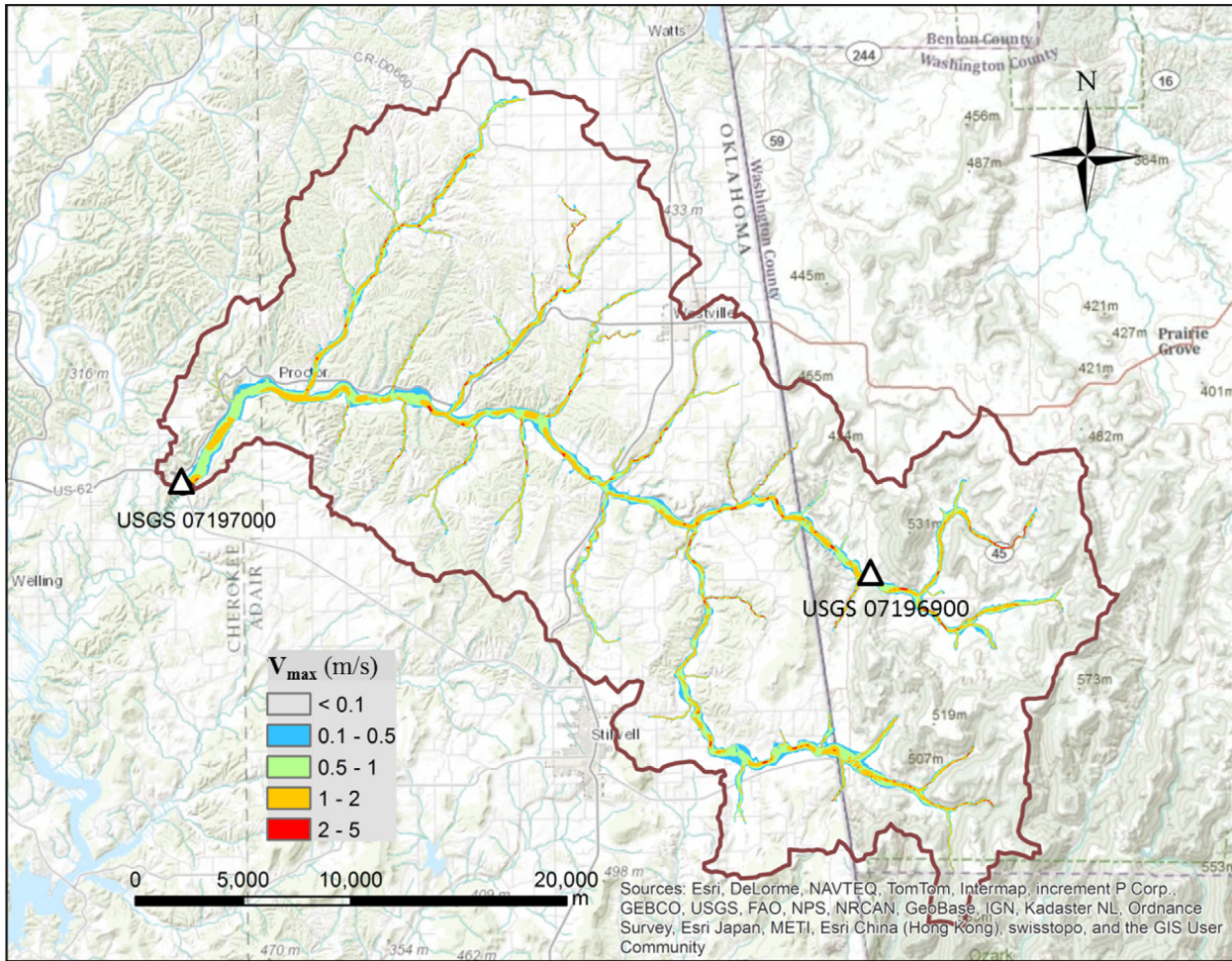


Fig. 9. Flow velocity (m/s) in baseline scenario (see specifications of baseline scenario in Table 2), forced with synthetic precipitation. V_{max} (m) is the maximum flow velocity in the simulation.

3. Case study, data collection and statistical metrics

3.1. Case study

Baron Fork at Eldon, Oklahoma (NWS forecast point ELDO2, Fig. 3) was chosen as the study area because it can be seen as a flashy catchment and data is available from the Distributed Model

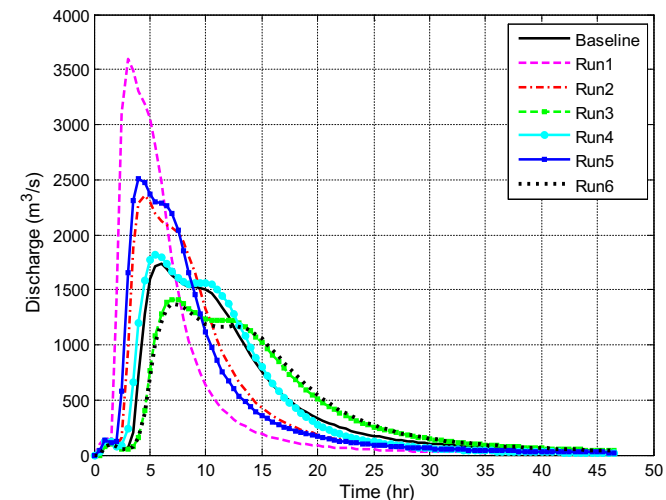


Fig. 10. Testing HiResFlood-UCI roughness parameter for Runs 1–6 listed in Table 2.

Intercomparison Project phase 2 (DMIP2, Smith et al., 2012a, 2012b). ELDO2 is an 808 km² catchment of the Baron Fork River on the border of Oklahoma and Arkansas. The USGS stream gauge 07197000 (latitude 35°55'16", longitude 94°50'18") is located at Eldon, Oklahoma. The USGS stream gauge 07196900 (latitude 35°52'48", longitude 94°29'11") is located at Dutch Mills, Arkansas, covering a drainage area of 105 km². ELDO2 is a natural watershed which has limited manmade raised linear features such as levees, roadways, and railways.

3.2. Data collection

Topographic data is crucially important in flood modeling (Sanders, 2007). One of the strongest limitations when using standard Digital Elevation Models (DEMs) in 2D hydraulic simulation is that they do not represent the riverbed topography information well. Sanders (2007) tested BreZo with various DEMs including Light Detection And Ranging (LiDAR), Interferometric Synthetic Aperture Radar (IfSAR), Shuttle Radar Topography Mission (SRTM), and National Elevation Dataset (NED) DEM at 3, 10, and 30 m. The author concluded that DEMs 10 m and 30 m could represent channel and overland flow when paired with numerical models but they may lead to underestimation of inundation area. Cook and Merwade (2009) also found that the flooded-area map reduces with higher resolution and better vertical accuracy in topographic data. Kim et al. (2012) used 50 m DEM and found value in their simulations as they relate to flood inundation. In this research,

Table 3
Testing HiResFlood-UCI hydraulic roughness sensitivity (see Scenario description in Table 2).

Scenario	H_{max} (m)	V_{max} (m/s)	Peak flow (m^3/s)	RMSE (m^3/s)	BIAS (-)	CORR (-)	NSE (-)	CSI (-)	POD (-)	FAR (-)
Baseline	10.25	5.69	1733.47	–	–	–	–	–	–	–
Run 1	10.26	9.04	3593.42	793.04	0.026	0.497	-1.093	0.900	0.901	0.001
Run 2	10.19	6.93	2362.20	341.73	0.013	0.870	0.611	0.958	0.959	0.000
Run 3	10.44	4.22	1414.13	203.55	-0.004	0.932	0.862	0.978	1.000	0.022
Run 4	10.64	9.04	1822.03	92.07	0.021	0.991	0.972	0.942	0.950	0.009
Run 5	10.39	6.02	2504.80	435.10	0.011	0.794	0.370	0.960	0.963	0.004
Run 6	10.59	5.69	1368.55	225.04	-0.004	0.916	0.831	0.975	1.000	0.024

DEM data at 10 m and 30 m resolution based on NED was downloaded from USGS NHD (<http://viewer.nationalmap.gov/viewer/nhd.html?p=nhd>). The 10 m and 30 m DEMs have vertical accuracies of ± 1.55 m and ± 2.44 m root mean square error (RMSE) respectively (Gesch et al., 2014).

The DMIP2 project (http://www.nws.noaa.gov/oh/hrl/dmip/2/data_link.html) offers projection and boundary shape files to extract ELDO2 catchment.

Forcing data for the model include next generation radar – NEXRAD rainfall data from DMIP2, Stage IV rainfall data from NCEP and temperature data from the North America Land Data Assimilation System (NLDAS, <http://ldas.gsfc.nasa.gov/nldas>).

Hourly streamflow data from 2000 to 2011 at the U.S. Geological Survey (USGS) stream gauge 07197000 was retrieved from USGS’s National Water Information System (NWIS, <http://nwis.waterdata.usgs.gov/nwis/>) for calibration and validation based on the streamflow at the watershed outlet. The 15-min streamflow and gauge height data at USGS 07196900 (available from 2007) was downloaded from NWIS for validating the predicted streamflow and flood stage at the interior point of the watershed.

3.3. Statistical metrics

The model was validated across the time periods of extreme flood events (excluding the time of calibration process) using four metrics: Root Mean Square Error (RMSE), BIAS, Pearson correlation coefficient (CORR) and Nash–Sutcliffe Efficiency (NSE).

$$RMSE = \sqrt{\frac{1}{n} \sum_{t=1}^n (q_o(t) - q_s(t))^2} \quad (3)$$

where n is the total number of observations, q_o is the observed discharge (m^3/s), and q_s is the simulated discharge (m^3/s) for each time step t .

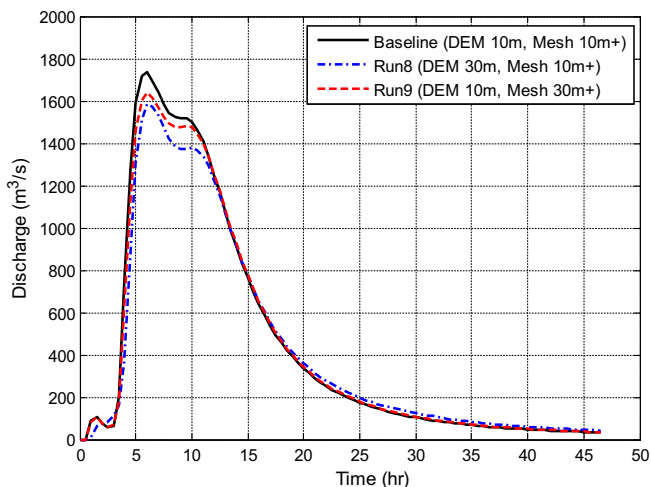


Fig. 11. Testing HiResFlood-UCI with DEM 30 m resolution and Mesh 30 m+ resolution.

BIAS indicates the tendency of the simulated flows in comparison with gauge observations. A BIAS of 0 is optimal. Positive values indicate an overestimation while negative values indicate a tendency to underestimate.

$$BIAS = \frac{\sum_{t=1}^n (q_s(t) - q_o(t))}{\sum_{t=1}^n q_o(t)} \quad (4)$$

CORR is the most commonly used measure for evaluating the goodness of fit of two hydrographs (McCuen and Snyder, 1975). CORR ranges from -1 (negatively correlated) to 1 (correlated). The ideal value of CORR is 1 and CORR of 0 indicates no correlation between the hydrographs.

$$CORR = \frac{\sum_{t=1}^n (q_o(t) - \bar{q}_o) \sum_{t=1}^n (q_s(t) - \bar{q}_s)}{\sqrt{\sum_{t=1}^n (q_o(t) - \bar{q}_o)^2} \sqrt{\sum_{t=1}^n (q_s(t) - \bar{q}_s)^2}} \quad (5)$$

where \bar{q}_o is the mean value of observed discharge, and \bar{q}_s is the mean value of simulated discharge.

NSE is used to assess the predictive power of the model. The ideal value of NSE is 1. Negative NSE values indicate that the mean of observations is a better predictor than the model.

$$NSE = 1 - \frac{\sum_{t=1}^n (q_s(t) - q_o(t))^2}{\sum_{t=1}^n (q_o(t) - \bar{q}_o)^2} \quad (6)$$

The unique advancement of the model is its capability to produce the spatio-temporal distribution of water flow in the channel/river network as well as in their flood plains in high resolution. The spatial outputs (flooded-area maps, flow velocity) from the model in an unstructured triangular cell mesh were regridded into a regular grid of 10 m \times 10 m for comparison. Three main metrics (Probability Of Detection – POD, False-Alarm Ratio – FAR, and Critical Success Index – CSI) were used with three statistics: hits (having flood in both simulation and observation), misses (flood in observation but not in simulation) and false alarms (flood in simulation but not in observation). For these spatio-temporal experiments, no areal observations are available. With that, they are used only for the sensitivity tests, taking the baseline run using calibrated HL-RDHM parameters, average values from Chow’s look-up table for channel and floodplain Manning n roughness, DEM 10 m resolution and mesh 10 m+ resolution (see description of baseline run in Table 2) as the “observation”.

POD indicates the fraction of observed floods that were correctly simulated. POD ranges from 0 to 1. POD of 1 means that floods were correctly simulated; 0 means no flooding detected by the model.

$$POD = \frac{\text{hits}}{\text{hits} + \text{misses}} \quad (7)$$

FAR measures the fraction of simulated flooding that was not associated with observation. Similar to POD, FAR of 1 indicates that all floods were not associated with observation, FAR of 0 indicates that no simulated floods found in observation.

$$FAR = \frac{\text{false alarms}}{\text{hits} + \text{false alarms}} \quad (8)$$

Table 4
Testing HiResFlood-UCI with DEM 30 m resolution (Run 8) and mesh 30 m+ resolution (Run 9, see scenario description in Table 2).

Scenario	H_{\max} (m)	V_{\max} (m/s)	Peak flow (m^3/s)	RMSE (m^3/s)	BIAS (-)	CORR (-)	NSE (-)	CSI (-)	POD (-)	FAR (-)
Baseline	10.25	5.69	1733.47	–	–	–	–	–	–	–
Run 8	12.43	6.09	1583.30	81.23	-0.039	0.993	0.978	0.714	0.850	0.183
Run 9	10.07	6.65	1636.67	33.08	-0.017	0.999	0.996	0.839	0.992	0.155

CSI measures the skill of the system ranging from 0 meaning no skill to 1 meaning perfect skill:

$$\text{CSI} = \frac{\text{hits}}{\text{hits} + \text{misses} + \text{false alarms}} \quad (9)$$

4. Model set up for ELDO2 catchment

4.1. Setting up HL-RDHM component

HL-RDHM version 3.2.0 was set up for the ELDO2 catchment. Distributed *a priori* parameter values of SAC-SMA model and Rutipix9 routing technique were adjusted by a set of calibrated coefficients provided by NWS. The model was set at 1 HRAP resolution (i.e. ~ 4 km) and an hourly time step to produce basin outlet and interior point time-series discharges, and gridded surface flow.

4.2. Setting up BreZo component

A new framework was proposed to design an efficient mesh for BreZo which allows for modeling large domains. First, ELDO2 was extracted from the DEM map of Illinois River basins (Fig. 4). ESRI ArcGIS terrain processing tools were used for watershed delineation to derive the stream network and 119 sub-catchments. Sub-catchment centroids were created and then snapped into the nearest stream serving as the subcatchment hydrograph point sources (Fig. 5).

To set up the unstructured triangular mesh, four zones based on the distance from the stream were created using buffering tools in ArcGIS (Table 1 and Fig. 6). Two meshes were created in this experiment. The first mesh (Case 1) has the highest resolution of 10 m while the other (Case 2) was designed with the highest resolution of 30 m.

ArcGIS interpolation tools and the Triangle software (Shewchuk, 1996) were used with the refinement option based on cell areas (Table 1) to create the final mesh (Fig. 7).

In terms of an efficient mesh, the final 10 m + resolution mesh (Case 1) has 802,405 elements and is significantly more efficient compared to the mesh of 25,589,112 elements designed with a uniform 10 m resolution. This leads to an approximately 32-fold reduction in computational time. It takes about 1 h to complete a 7 h simulation for this experiment on a 16-core computing node of the NCAR's Yellowstone cluster.

5. Testing HiResFlood-UCI with synthetic input

5.1. Scenario description for synthetic input

This experiment used a uniform synthetic rainfall input of 2 continuous hours of 87.38 mm/hr created from the Partial Duration Series (PDS)-based precipitation frequency estimates with 90% confidence intervals for 2 h, 1% probability at USGS 7197000.

The precipitation was uniformly spatially distributed over the catchment in an attempt to negate effects that natural, distributed precipitation will have on discharge, particularly on the timing of events. The main purpose of using synthetic data in this experiment is to capture the impact of changing certain model elements

such as channel and floodplain roughness (Manning n), DEM resolution, mesh resolution, and calibration of the hydrologic model. Table 2 highlights the various model runs that were used to explore model response to changes in the aforementioned model components.

The baseline run employs the average Manning n value for the channel and floodplain as provided by Chow (1959), uses the calibrated hydrologic model parameters as provided by the NWS, a 10 m DEM, and a mesh resolution with the finest grids near the river at a 10 m resolution (Case 1 in Table 1).

Significant attention was given to the evaluation of roughness parameter choice because of the potential tradeoffs of having different floodplain and channel roughness. In fact, this parameter is often used to compensate the lack of information about the channel. Runs 1–6 explore combinations of high and low parameter values in both the channel and the floodplain in an effort to examine the entire spectrum of possible outcomes that may result from a possibly uninformative roughness choice.

Run 7 addresses the outcome of using the *a priori* parameter grids for HL-RDHM (based on soil surveys) rather than calibrated grids. This is a realistic scenario in that some basins may not have a stream gauge at the outlet to allow for calibration of the hydrologic model. Run 8 explores the outcome of using a 30 m DEM grid as the base for generating the mesh, which is currently the finest resolution available in many parts of world. Run 9 investigates the use of a slightly coarser mesh with the finest grids at 30 m. It should be noted that although the option to consider even coarser mesh resolution exists, the main intent of this work to provide high resolution flood information begins to deteriorate with a mesh coarser than 30 m.

5.2. Model results for synthetic input

One major innovation of HiResFlood-UCI is the capability to generate and display distributed high resolution flow information

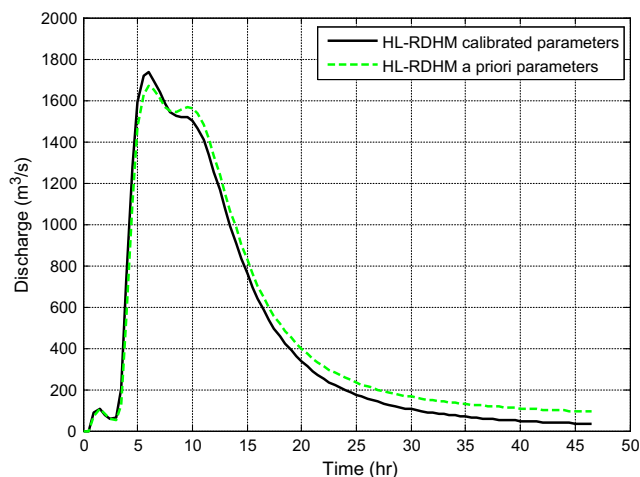


Fig. 12. Testing HiResFlood-UCI with HL-RDHM *a priori* parameters which were derived from soil types and land uses.

Table 5Testing HiResFlood-UCI with HL-RDHM *a priori* parameters (Run 7, see scenario description in Table 2).

Scenario	H_{\max} (m)	V_{\max} (m/s)	Peak flow (m^3/s)	RMSE (m^3/s)	BIAS (-)	CORR (-)	NSE (-)	CSI (-)	POD (-)	FAR (-)
Baseline	10.25	5.69	1733.47	–	–	–	–	–	–	–
Run 7	10.34	5.46	1670.70	65.13	0.093	0.996	0.986	0.991	0.998	0.007

for an entire basin. Fig. 8 shows the resulting map of maximum flow depth for the baseline simulation using synthetic precipitation as input. The corresponding maximum flow velocity map for the baseline run is shown in Fig. 9.

5.2.1. Hydraulic roughness parameter sensitivity (Runs 1–6)

The outcomes of the hydraulic roughness parameter sensitivity tests for the synthetic precipitation experiment point to the importance of careful identification of the roughness parameter in both the channel and floodplain (Fig. 10 and Table 3). This is particularly evidenced through the evaluation of Runs 4 and 5 (minimum channel roughness, maximum floodplain roughness and vice versa respectively) – see Table 2. While the effect of changing the roughness parameters is more substantial in Run 5, both runs had the same outcome of an increasing peak, an earlier timing of the peak, and a steepening of the recession limb. This suggests that neither parameter significantly dominates the other, thus accurate characterization of both is important. Not surprising are the hydrographs resulting from Runs 1 and 6. Run 1 utilizes the smallest Manning n for both the channel and floodplain and intuitively features a hydrograph with a sharp peak and a quickly descending recession limb. Accordingly, Run 6 shows the opposite with the smallest, most drawn-out peak of all runs as it uses the highest roughness parameters.

5.2.2. Testing HiResFlood-UCI with Run 8 (DEM 30 m resolution) and Run 9 (Mesh 30 m+ resolution)

Of the three sensitivity tests investigated other than the Manning n roughness sensitivity, the one that had the most negative impact on the resulting area-based statistics was decreasing the DEM resolution from 10 m to 30 m. This decrease in quality of flood extent-based metrics is intuitive for an increase in DEM resolution as the hydraulic model relies heavily on topography to govern flood dynamics. While this scenario suffered the worst area-based statistics compared to the other sensitivity tests, the quality reduction was not so severe that it would warrant not using the coupled system if only a 30 m were available. The point-based outlet statistics suggest the same, as the NSE remains near 1 and the BIAS is the lowest compared to the other two non-roughness sensitivity runs.

The mesh resolution sensitivity test suggests there is little change compared to the baseline scenario, especially in terms of outlet statistics, when the mesh resolution was increased from 10 m+ to 30 m+ (Fig. 11 and Table 4). Not surprisingly, POD is slightly lower than 1 and FAR is slightly higher than 0. It is unreasonable to expect a coarser mesh to perfectly capture the details of a finer mesh. However, the differences are quite small for this synthetic study, and when modeling very large basins, it may be necessary to use a 30 m+ mesh rather than a 10 m+ mesh to save

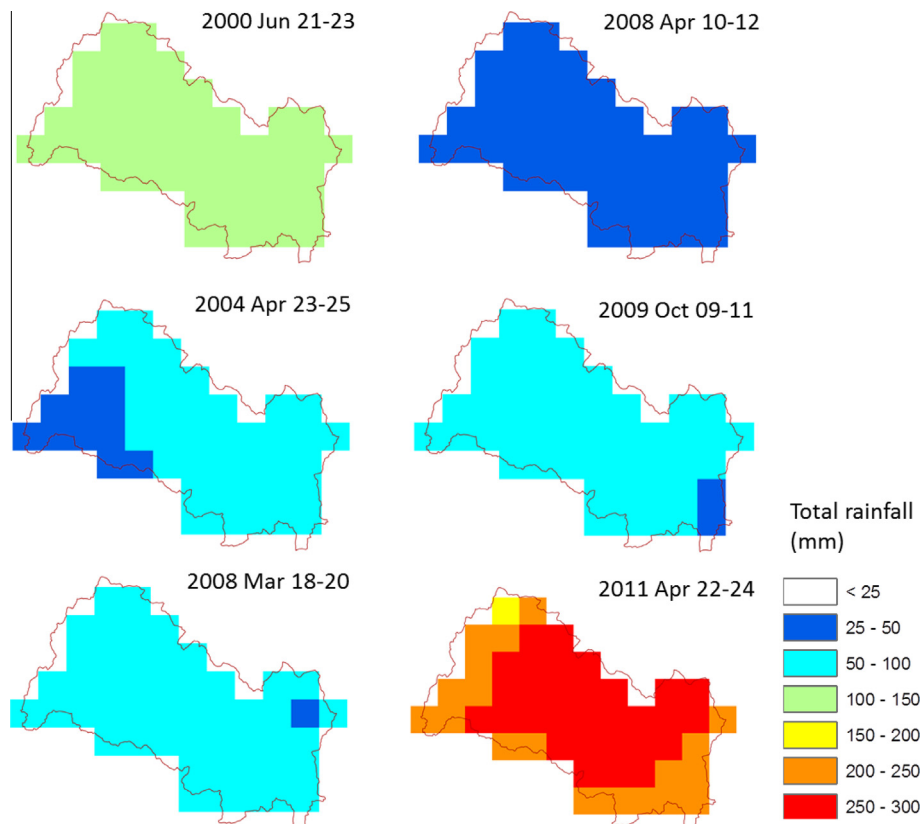


Fig. 13. Total Stage IV rainfall (mm) of extreme events in ELD02 from 2000 to 2011.

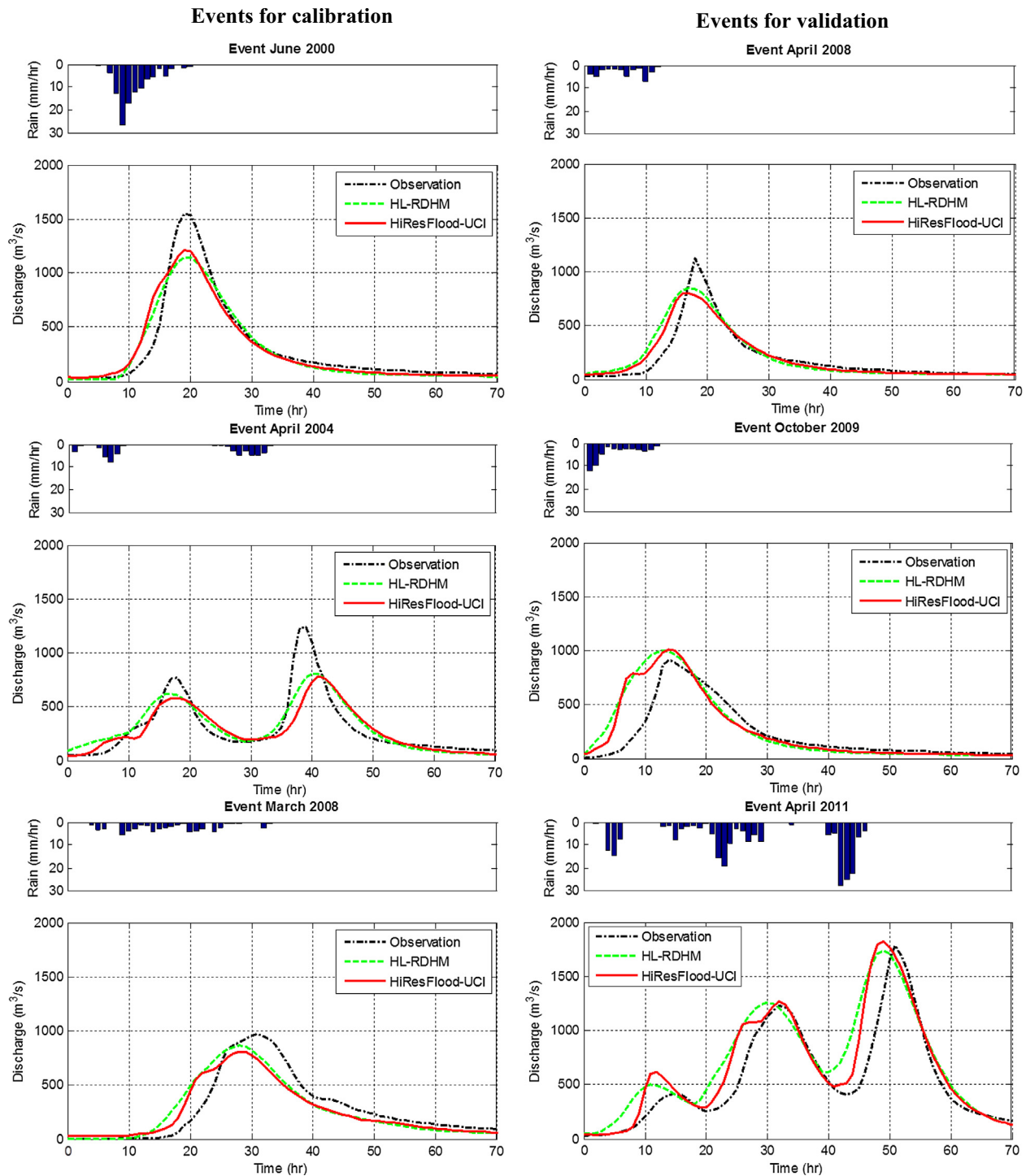


Fig. 14. HiResFlood-UCI simulation results at watershed outlet (events June 2000, April 2004 and March 2008 for model calibration; events April 2008, October 2009 and April 2011 for model validation).

computational expenses. This aspect of the sensitivity analysis suggests that a 30 m+ mesh would not be unreasonable for use, particularly in very large basins.

5.2.3. Testing HiResFlood-UCI with HL-RDHM *a priori* parameters (Run 7)

When the hydrologic model is run using *a priori* parameter grids as opposed to those calibrated for the DMIP2 experiment, the overall impact on basin discharge is minimal in the synthetic precipitation experiment (Fig. 12 and Table 5). Peak timing is unchanged

and only a slight reduction of the first major peak and a slight increase of the secondary peak are noticeable. Additionally, the tail of the recession limb becomes slightly fatter compared to that of the baseline run. Although anecdotal, the low sensitivity of the coupled model system to using *a priori* parameter grids for the hydrologic model rather than calibrated grids is encouraging. There are some cases where basins are ungauged, and calibration of the hydrologic model component using discharge observations is impossible. The results show that, for at least this basin, the inability to further calibrate the *a priori* parameter grids does not

Table 6

Statistics of simulations by HL-RDHM and HiResFlood-UCI at watershed outlet. The events in June 2000, April 2004 and March 2008 were used for model calibration (in shade).

Event	Observation/Simulation	Peak flow (m ³ /s)	Peak flow error (%)	Phase error (hr)	RMSE (m ³ /s)	BIAS (-)	CORR (-)	NSE (-)
June 2000	Observation	1548.90	-	-	-	-	-	-
	HL-RDHM	1144.30	-26.12	1	116.76	-0.087	0.963	0.914
	HiResFlood-UCI	1200.00	-21.76	0	122.79	-0.062	0.956	0.905
April 2004	USGS Observation	1234.60	-	-	-	-	-	-
	HL-RDHM	808.40	-34.52	1	124.99	0.004	0.904	0.800
	HiResFlood-UCI	756.27	-36.70	2	159.92	-0.067	0.830	0.673
March 2008	Observation	971.27	-	-	-	-	-	-
	HL-RDHM	862.79	-11.17	-3	129.58	-0.057	0.900	0.807
	HiResFlood-UCI	813.00	-16.29	-3	122.14	-0.092	0.919	0.839
April 2008	Observation	1121.30	-	-	-	-	-	-
	HL-RDHM	851.63	-24.05	-1	100.87	0.071	0.914	0.825
	HiResFlood-UCI	762.00	-28.66	-1	87.00	-0.018	0.933	0.870
October 2009	Observation	911.80	-	-	-	-	-	-
	HL-RDHM	996.37	9.28	-1	179.10	0.173	0.835	0.507
	HiResFlood-UCI	976.00	10.77	0	163.69	0.149	0.853	0.588
April 2011	Observation	1781.10	-	-	-	-	-	-
	HL-RDHM	1740.10	-2.30	-2	260.11	0.253	0.888	0.665
	HiResFlood-UCI	1840.00	2.18	-2	210.93	0.176	0.925	0.780

significantly depreciate the overall quality of the coupled system. This sentiment is echoed in other applications of HL-RDHM that found reasonable results using the *a priori* parameter sets including Koren et al. (2003) and Reed et al. (2004). Reed et al. (2007) found that error statistics from calibrated simulations were similar to or showed modest improvement over uncalibrated runs.

6. Model application

6.1. Experiment setup for real events

The HiResFlood-UCI model was implemented for 6 real flooding events in the ELDO2 basin. These events were selected based on the

highest observed streamflow for which precipitation data were concurrently available. Garambois et al. (2014) have shown a robust medium catchment behavior can be captured when multiple events are used in the calibration process. The flooding events in June 2000, April 2004, and March 2008 were selected as calibration runs for BreZo, and 3 additional events (April 2008, October 2009, and April 2011) were run as validation events. Fig. 13 highlights the total precipitation distribution of each of these events as they appear on the HRAP grid. The selected precipitation events represent a range of possible storm types, allowing for insight into how the models react given different scenarios. March 2008 and April 2008 represent lighter but longer storms, whereas June 2000 and April 2011 have much more intense and generally shorter

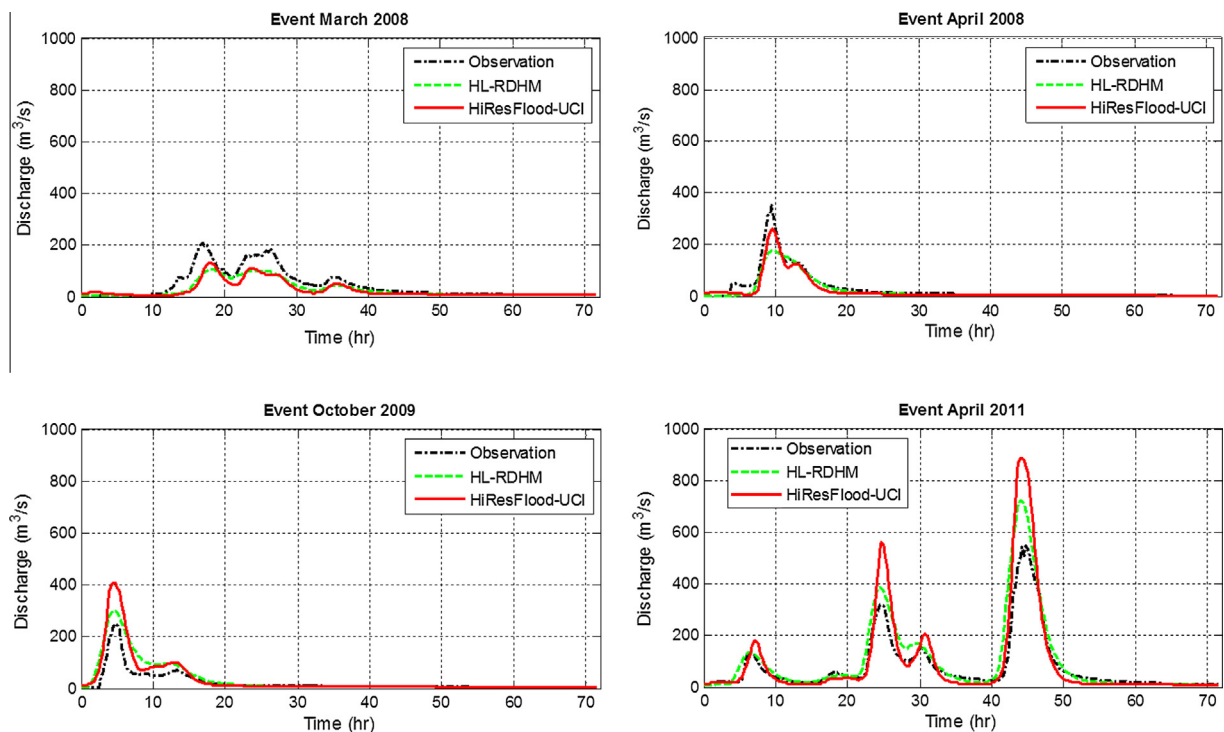


Fig. 15. HiResFlood-UCI simulation results at interior point USGS 07196900.

Table 7
Statistics of simulations by HL-RDHM and HiResFlood-UCI at interior point USGS 07196900.

Event	Observation/simulation	Peak flow (m ³ /s)	Peak flow error (%)	Phase error (hr)	RMSE (m ³ /s)	BIAS (-)	CORR (-)	NSE (-)
March 2008	USGS Observation	208.41	–	–	–	–	–	–
	HL-RDHM	104.92	–49.66	1.50	30.12	–0.383	0.951	0.675
	HiResFlood-UCI	129.03	–38.09	1.25	33.22	–0.422	0.918	0.605
April 2008	USGS Observation	353.96	–	–	–	–	–	–
	HL-RDHM	177.22	–49.93	0.00	23.70	–0.251	0.944	0.825
	HiResFlood-UCI	260.55	–26.39	0.00	17.83	–0.250	0.974	0.901
October 2009	USGS Observation	251.74	–	–	–	–	–	–
	HL-RDHM	300.50	19.37	–0.25	29.60	0.499	0.945	0.440
	HiResFlood-UCI	407.21	61.76	–0.25	37.77	0.523	0.977	0.089
April 2011	USGS Observation	546.51	–	–	–	–	–	–
	HL-RDHM	721.90	32.09	–0.50	57.10	0.274	0.967	0.734
	HiResFlood-UCI	885.94	62.11	–0.75	77.65	0.206	0.974	0.509

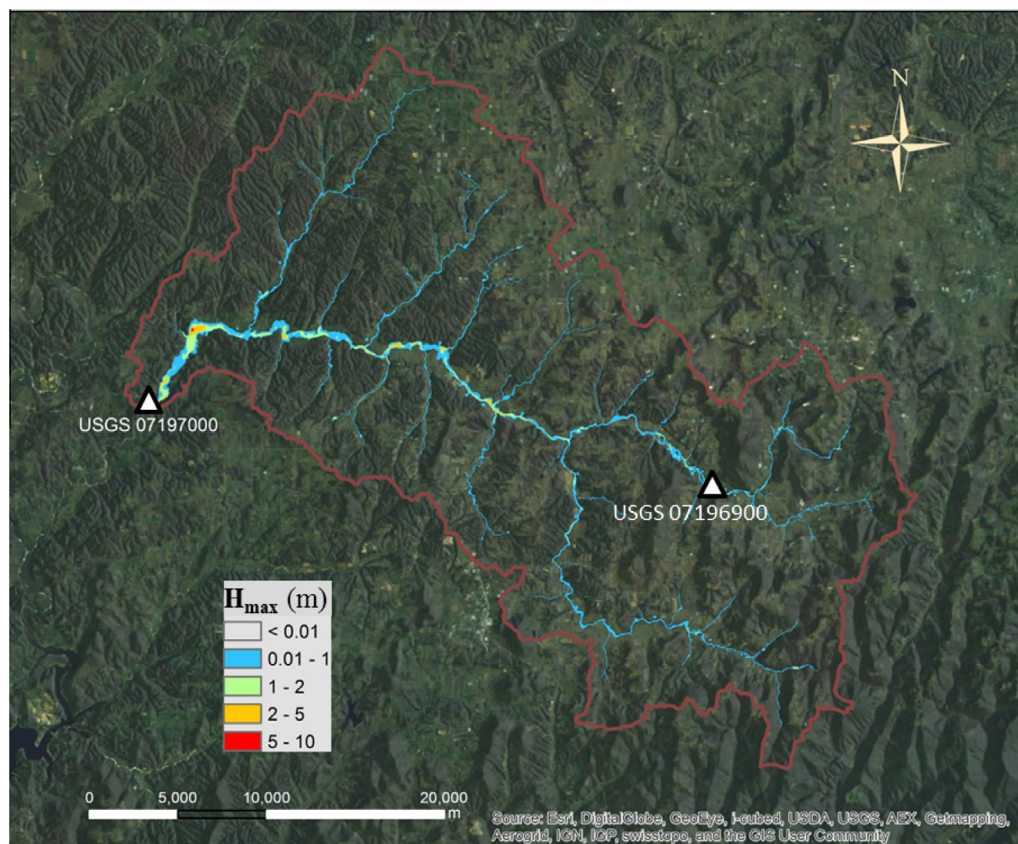


Fig. 16. HiResFlood-UCI simulated flooded-area map of ELDO2 in extreme event in April 2011.

storms. Additionally, some storms are multimodal (April 2004 and April 2011), while others are a more continuous events. The hydrographs in Fig. 14 depict the various storm events.

BreZo component was initialized for each event with a warm-up run that provides a low flow discharge similar to the watershed outlet observed discharge at the beginning of the simulation. These events were also simulated using the NWS standard HL-RDHM with its native routing scheme rather than BreZo. This is an important investigation to make certain that the vital added information gained from using HiResFlood-UCI such as flow velocity, depth, and areal flood extent, do not compromise the quality of the point discharge information that HL-RDHM already provides.

Hourly 4 km NEXRAD radar rainfall data from 1995 to 2001 over the basin was from DMIP2. The National Centers for Environmental Prediction/Environmental Modeling Center (NCEP/EMC) hourly 4 km Stage IV rainfall data from 2002 to 2011 for the entire CONUS was downloaded from the National center for Atmospheric Research (NCAR) website (<http://data.eol.ucar.edu/codiac/dss>). The temperature data in this experiment is from NLDAS.

Manual calibration of the Manning n values was conducted for the floodplain and river channel. Calibration efforts were based on optimizing the average NSE (3 calibration events) to the optimal value of 1 for the outlet hydrograph. This resulted in a channel roughness value of $n_1 = 0.05$ and a floodplain roughness of $n_2 = 0.11$, and yielded an average NSE of 0.806. These roughness

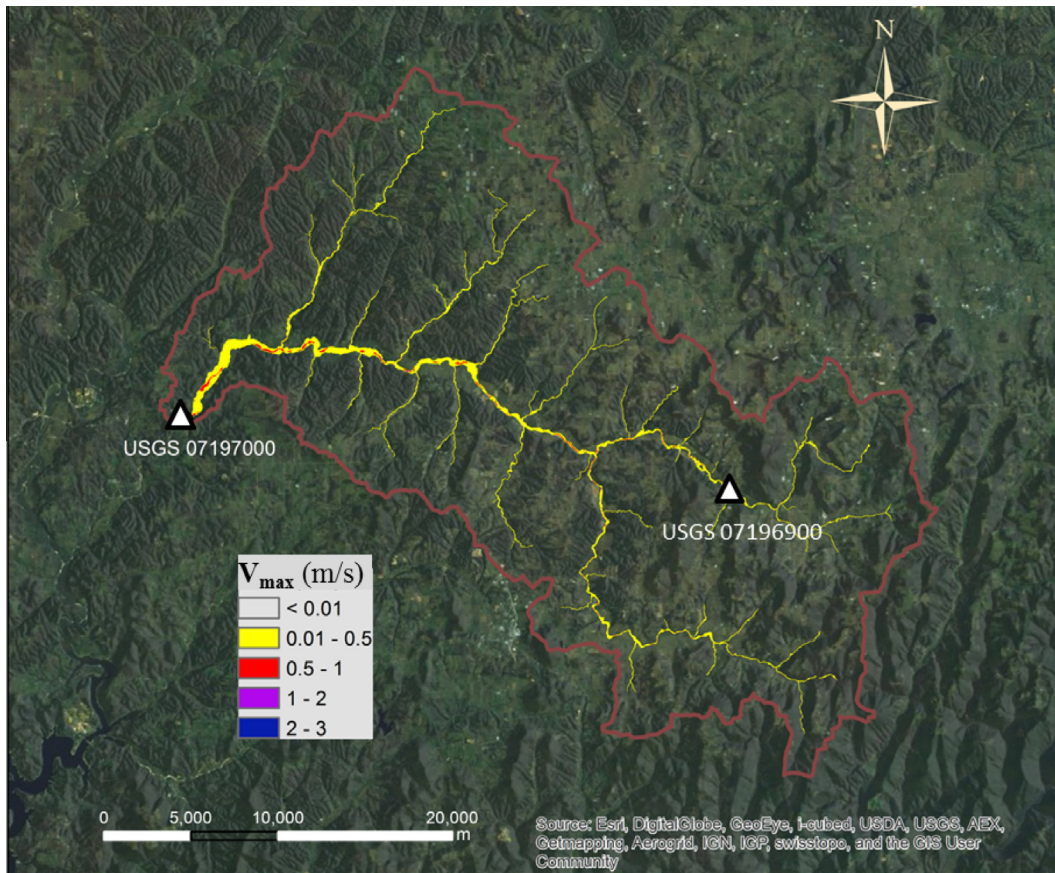


Fig. 17. HiResFlood-UCI simulated flow velocity of ELDO2 in extreme event in April 2011.

parameter values were subsequently used in the remaining three validation flood events.

6.2. Model results for real events

6.2.1. Discharge at the watershed outlet

The simulated hydrographs at the outlet for the 6 case studies (Fig. 14) show that HiResFlood-UCI performs comparably to HL-RDHM when it comes to producing flood peak magnitude, and the peak timing only differed by at most 2 h. The events chosen for calibration and validation offer a wide variety of storm types, which in turn, produce different hydrograph responses. The storms in April 2004 and 2011 have two and three distinct precipitation events respectively that result in multiple peaks in the streamflow response. In general, peak timing was a little early for the three peaks in the April 2011 simulation, but the peak magnitudes were represented reasonable well. In contrast, the April 2004 simulations had a slight delay in peak timing and the highest peak flow error for all simulated events. The simulation of the single peak events largely featured early peak phase timing, and generally underestimated. The event in October 2009 shows a substantially premature rise in the hydrograph prior to the main peak that was observed. It is understood that this is due to a collection of factors including errors related to the model itself, but also those associated with model input (especially precipitation). Table 6 summarizes the statistics of the case studies for both models with the USGS gauge at the ELDO2 outlet serving as the “true” observation. In all of the selected cases, the statistics for HL-RDHM are quite similar to those of HiResFlood-UCI, and no one model decisively dominates the other. This is an encouraging result as the

coupled model is able to provide additional information, particularly spatially distributed high resolution flow depth and velocity while at the same time not sacrificing the quality outlet flow information that the native hydrologic model was designed to generate.

6.2.2. Discharge at interior point

Since the USGS stream gauge 07196900 at Dutch Mills was installed in 2007 as part of DMIP2 project, the observed streamflow is available for validation at the interior point for only 4 events in March and April 2008, October 2009 and April 2011. Fig. 15 and Table 7 show the similarity in statistics between the discharges of the four events at the interior point simulated by HiResFlood-UCI and the original HL-RDHM. It is noted that both HL-RDHM and HiResFlood-UCI were calibrated for the ELDO2 outlet discharge, not for the discharge at the interior point. Also, the main purpose of HiResFlood-UCI is to provide more information about flash floods (flooded maps and flow velocity), not to necessarily provide better simulated hydrographs. The results suggest that HiResFlood-UCI is capable of preserving the ability of the distributed hydrologic model HL-RDHM to simulate streamflow at interior points of the watershed.

6.2.3. Flooded maps and flow velocity

Figs. 16–18 highlight the spatial distribution of the maximum water depth (H_{max}) and velocity for each pixel in the ELDO2 catchment for the April 2011 event. The value of HiResFlood-UCI is exemplified by this series of figures in that they provide a clear picture of the most extreme depth and velocity for the entire basin

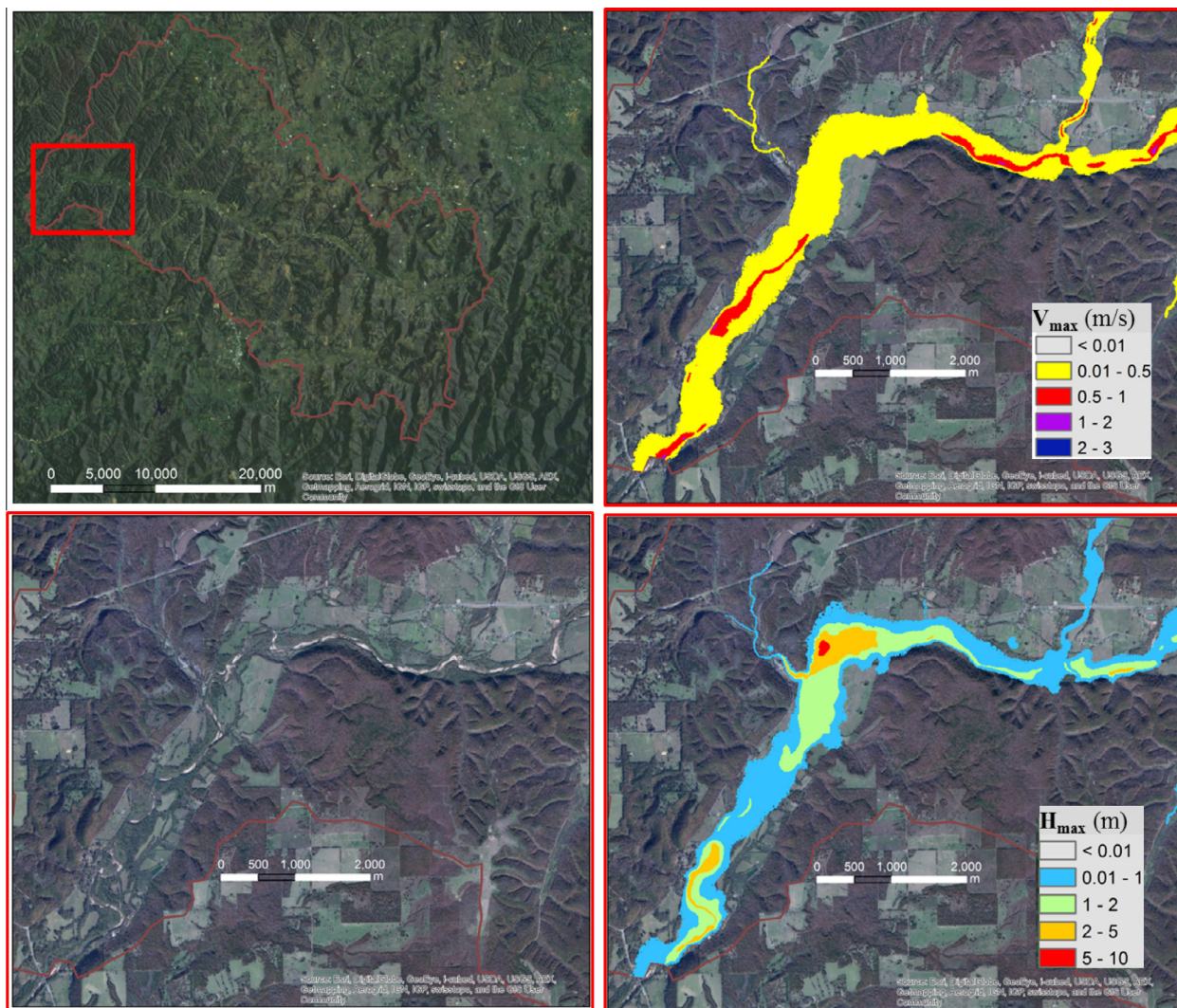


Fig. 18. A sample of a detailed flooded area map and flow velocity in ELD02 watershed for an event in April 2011 provided by HiResFlood-UCI.

(Figs. 16 and 17), but maintain a high enough resolution such that highly localized impacts (i.e. flooding of individual fields) can be seen (Fig. 18). While some existing models (e.g. MIKE FLOOD, BreZo) are capable of capturing inundation at high resolutions, often it is only of a river reach or a very small catchment due to computational expense. The coupled structure of HiResFlood-UCI allows for efficient production of high resolution, spatial flow information for the whole catchment. While for some events, the estimated hydrograph from HiResFlood-UCI may be similar to that of HL-RDHM, the HiResFlood-UCI provides important information such as flow depth and velocity that is not available from commonly used hydrologic models. Flow depth and velocity are very important for flood warning, and the proposed HiResFlood-UCI can potentially be used to enhance NWS's flood warning capabilities.

6.2.4. Estimation of the validity of flooded maps using observed gauge height

Validation of the flooded maps was performed at a USGS gauge located at an interior point of the ELD02 catchment (Fig. 19). A cross section of the channel at the gauge location was constructed from a 10 m DEM, with elevation being relative to the datum of the gauge. Simulated flood stage was retrieved using the flood extent

maps and flow depth information produced by HiResFlood-UCI in conjunction with the channel cross section.

The simulated and observed flood stage of the four validation events at the interior point are shown in Fig. 20. While the difference between simulated and observed flood stage is substantial for all events (40–70% error or 1.81–2.08 m), the simulation error is significantly reduced during flood peaks (5–29% error or 0.19–0.82 m). Table 8 summarizes the flood peak stage and event stage errors for each of the validation events. Large errors in stage height for low flow periods at this site are not unexpected, as the 10 m DEM remains too coarse to capture the fine details of this small stream. This smoothing of channel geometry greatly impacts simulations of this small tributary during low flows, and presents a limitation of the model to represent stage height in such situations. The process of adjusting Manning's roughness in tandem with using the high-resolution mesh is one way this coupled system is able to compensate for a lack of topographical information, particularly channel geometry. Regardless, the simulated stage greatly improved during flooding, as depths of high flows become less susceptible to cross section geometry. The flooding period is the most important period for HiResFlood-UCI because the model's purpose is to capture details of high flow events.

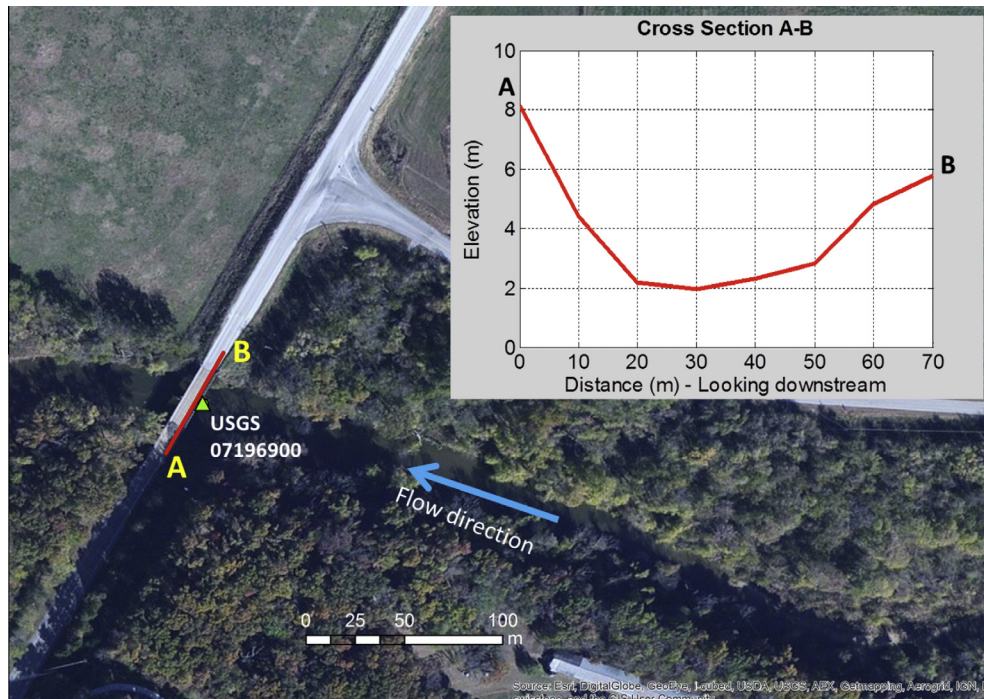


Fig. 19. USGS 07196900 gauge station site. Cross section derived from 10 m DEM at gauge USGS 07196900, elevation with respect to the gauge datum (300.676 m National Geodetic Vertical Datum of 1929, NGVD29).

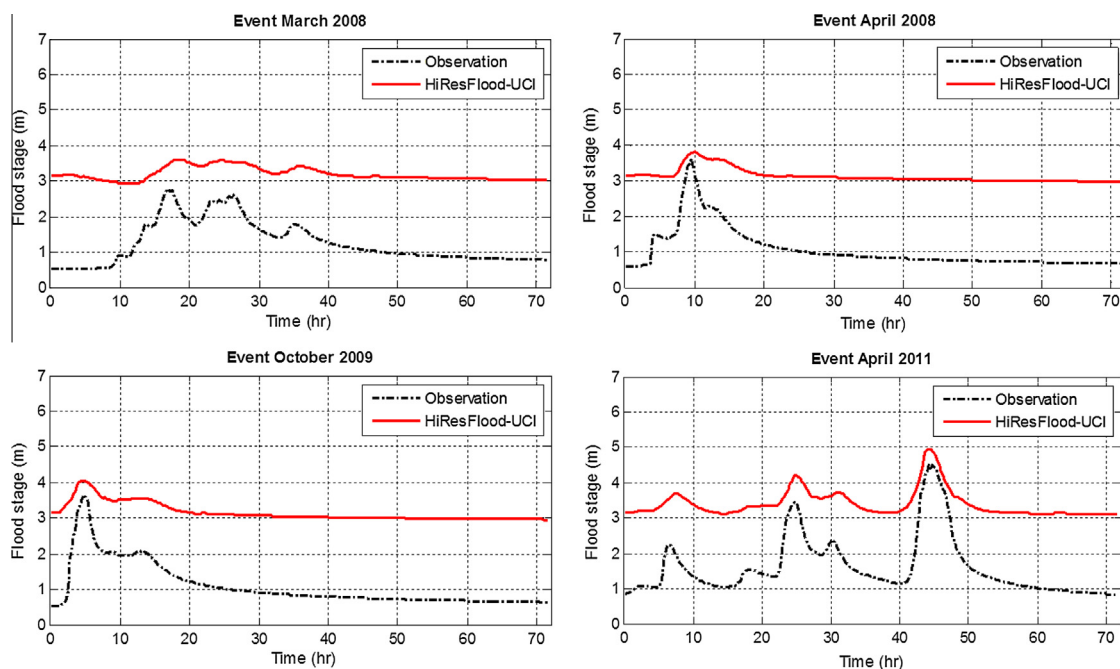


Fig. 20. Flood stage (m) from HiResFlood-UCI and USGS measurements with respect to the datum of gauge USGS 07196900 (300.676 m NGVD29).

7. Conclusion and future direction

A coupled hydrologic–hydraulic model for flash flood modeling called HiResFlood-UCI was developed. The system was designed to combine the strengths of the NWS HL-RDHM distributed hydrologic model with those of the BreZo 2D hydraulic model. A

semi-automated technique of unstructured mesh generation was developed to cluster an adequate density of computational cells along rivers such that numerical errors are negligible compared with other sources of error, but no more so that computational costs of the hydraulic model are kept to the bare minimum.

Table 8

Statistics of flood stage simulated by HiResFlood-UCI with respect to the datum of gauge USGS 07196900.

Event	Observation/simulation	Flood stage (m)	Flood stage error (m)	Event stage error (m)
March 2008	USGS Observation	2.78	–	–
	HiResFlood-UCI	3.60	0.82	1.94
April 2008	USGS Observation	3.63	–	–
	HiResFlood-UCI	3.82	0.19	2.08
October 2009	USGS Observation	3.64	–	–
	HiResFlood-UCI	4.04	0.40	2.06
April 2011	USGS Observation	4.51	–	–
	HiResFlood-UCI	4.96	0.45	1.81

The HiResFlood-UCI coupled hydrologic–hydraulic system was evaluated on several levels. Synthetic precipitation studies permitted investigation of various model aspects. Tests with calibrated versus *a priori* parameter grids for the hydrologic (HL-RDHM) component suggest that even with *a priori* parameter set, HiResFlood-UCI could still produce reasonable results. The roughness parameter for floodplain and channel in the hydraulic model (BreZo) component was evaluated using a range of roughness parameters and their combinations. The findings from this sensitivity test suggest that selection of channel and floodplain roughness should be done with care, as the model appears sensitive to these parameters. Additionally, no one roughness parameter dominated the other, and different combinations led to similar outlet flow results. Results when using coarser mesh resolution (30 m+) and DEM resolution (30 m) suggest that it is more imperative to have a high quality, high resolution DEM to derive the mesh, even if the mesh resolution is slightly coarser.

HiResFlood-UCI was also evaluated using 6 real precipitation events as model input. The primary outcome of these experiments shows that HiResFlood-UCI is able to produce spatially distributed, high resolution flow information without losing the quality hydrographs at both watershed outlet and interior point that HL-RDHM can already generate. These case studies also provide a look at how HiResFlood-UCI can produce high resolution for the entire basin rather than for just a limited reach. A unique advantage of HiResFlood-UCI over the current HL-RDHM is that in addition to the flow hydrograph it offers inundated areas, flow depth and velocity, which are fundamental to reliable flood warning. The model was also validated for the flooded map using USGS observed water level available at an interior point. The results show the predicted flood stage error is 0.82 m or less.

While initial development and implementation of HiResFlood-UCI has been completed, there are necessary on-going efforts toward validation of the spatial flow information that it provides. Such efforts include utilization of post flood surveys conducted by the USGS in which flood extent was directly measured in many locations of the same basin, and flow depth and velocity were independently determined. Aerial photos of flood events will also aid in the validation of flood extend for HiResFlood-UCI. These pursuits are already underway in an effort to verify the unique spatial information provided by this coupled hydrologic–hydraulic system. For example, HiResFlood-UCI has been applied for the Iowa flood 2008 and shows good agreement with flooded maps derived satellite imagery (Nguyen et al., 2015). Once HiResFlood-UCI has been tested for some selected catchments in the United States and shown promising results, it will be implemented for global scale using the UC Irvine's Precipitation Estimation from Remotely Sensed Information using Artificial Neural Networks – Cloud Classification System (PERSIANN-CCS, Hong et al., 2004) real-time high-resolution data and Global Forecast System (GFS) data for flash flood nowcast/forecast purposes.

Acknowledgements

This research was supported by NOAA Office of Hydrologic Development (OHD) National Weather Service (NWS) student research fellowship, and the Department of Defense (DoD) through the National Defense Science & Engineering Graduate Fellowship (NDSEG) Program. This work was also supported by the Cooperative Institute for Climate and Satellites (CICS) and the Army Research Office – United States (Award W911NF-11-1-0422). The first author was financially supported by the Vietnamese International Education Development program and the University of California, Irvine Chancellor Club for Excellence Fellowship while conducting this research. We would like to acknowledge high-performance computing support from Yellowstone (ark:/85065/d7wd3xhc) provided by NCAR's Computational and Information Systems Laboratory, sponsored by the National Science Foundation.

Appendix A. ELDO2 calibrated scalar adjustment factors for *a priori* parameters (provided by NWS)

Parameter	Description	Calibrated coefficient
sac_PCTIM	Minimum impervious area	0.001
sac_ADIMP	Additional impervious area	0.000
sac_RIVA	Riparian vegetation area	0.025
sac_SIDE	Ratio of non-channel baseflow to channel baseflow	0.000
sac_RSERV	Percent/100 of lower zone free water which cannot be transferred to lower zone tension water	0.300
sac_EFC	Effective forest cover	0.000
sac_UZTWM	Lower zone tension water capacity	–0.753
sac_UZFWM	Upper zone free water capacity	–0.509
sac_UZK	Fractional daily upper zone free	–0.710
sac_ZPERC	Maximum percolation rate	–8.342
sac_REXP	Exponent for the percolation equation	–0.753
sac_LZTWM	Lower zone tension water capacity	–0.628
sac_LZFMS	Lower zone supplemental free water capacity	–1.016
sac_LZFPM	Lower zone primary free water capacity	–1.148

Appendix A (continued)

Parameter	Description	Calibrated coefficient
sac_LZSK	Fractional daily supplemental withdrawal rate	−0.569
sac_LZPK	Fractional daily primary withdrawal rate	−0.494
sac_PFREE	Percent/100 of percolated water which always goes directly to lower zone free water storages	−0.357
rutpix_Q0CHN	Specific channel discharge per unit channel cross-section area	−0.900
rutpix_QMCHN	Power value in relationship between discharge and cross-section	−0.980

Appendix B. List of acronyms

Acronym	Description
BIAS	Bias
BreZo	2D hydraulic model
CARIMA	1D hydraulic model
CHRS	Center for Hydrometeorology & Remote Sensing at University of California, Irvine
CONUS	Contiguous United States
CORR	Pearson correlation coefficient
CSI	Critical Success Index
DEM	Digital Elevation Model
DHI	Danish Hydraulic Institute
DMIP2	Distributed Model Intercomparison Project phase 2
ELDO2	A catchment of the Baron Fork River on the border of Oklahoma and Arkansas
FAR	False-Alarm Ratio
GFS	Global Forecast System
HiResFlood-UCL	Coupled hydrologic–hydraulic model for flood simulation
HL-RDHM	Hydrology Laboratory – Research Distributed Hydrologic Model
HRAP	Hydrologic Rainfall Analysis Project
IfSAR	Interferometric Synthetic Aperture Radar
ISBA	Interactions between Soil–Biosphere–Atmosphere
LiDAR	Light Detection And Ranging
LISFLOOD-FP	2D hydrodynamic model
MIKE FLOOD	2D flood model
NED	National Elevation Data
NEXTRAD	Next generation radar
NHD	National Hydrology Dataset
NLDAS	North America Land Data Assimilation Systems
NOAA	National Oceanic and Atmospheric Administration
NSE	Nash–Sutcliffe Efficiency
NWS	National Weather Service
OFM	Overland Flow Model

Appendix B (continued)

Acronym	Description
OHD	Office of Hydrologic Development
PDS	Partial Duration Series
PERSIANN	Precipitation Estimation from Remotely Sensed Information using Artificial Neural Networks
PERSIANN-CCS	Precipitation Estimation from Remotely Sensed Information using Artificial Neural Networks – Cloud Classification System
POD	Probability Of Detection
RMSE	Root Mean Square Error
Rutpix9	Routing technique in HL-RDHM model
SAC-SMA	Sacramento – Soil Moisture Accounting model
Snow-17	Snow accumulation and ablation model
SRTM	Shuttle Radar Topography Mission
SWOT	Surface Water and Ocean Topography mission
TOPMODEL	1D hydraulic model
Triangle	Triangular mesh designing software
tRIBS	Triangulated Irregular Network–Real Time Integrated Basin Simulator model
UCI	University of California, Irvine
USACE	US Army Corps of Engineers
USGS	US Geological Survey
VIC	Variable Infiltration Capacity model

References

- Anderson, E.A., 1973. National Weather Service River Forecast System–Snow Accumulation and Ablation Model. Technical Memo. NOAA, Silver Spring, MD, pp. 217.
- Bates, P.D., Horritt, M.S., Fewtrell, T.J., 2010. A simple inertial formulation of the shallow water equations for efficient two dimensional flood inundation modelling. *J. Hydrol.* 387, 33–45.
- Begnudelli, L., Sanders, B.F., 2006. Unstructured grid finite-volume algorithm for shallow-water flow and scalar transport with wetting and drying. *J. Hydraulic Eng.* 132 (4), 371–384.
- Begnudelli, L., Sanders, B.F., 2007. Simulation of the St. Francis dam-break flood. *J. Eng. Mech.* 133 (11), 1200–1212.
- Begnudelli, L., Sanders, B.F., Bradford, S.F., 2008. Adaptive Godunov-based model for flood simulation. *J. Eng. Mech.* 134 (6), 714–725.
- Biancamaria, S., Bates, P.D., Boone, A., Mognard, N.M., 2009. Large-scale coupled hydrologic and hydraulic modelling of the Ob river in Siberia. *J. Hydrol.* 379, 136–150.
- Bonnifait, L., Delrieu, G., Laya, M.L., Boudevillain, B., Massonb, A., Belleudy, P., Gaume, E., Saulnier, G.M., 2009. Distributed hydrologic and hydraulic modelling with radar rainfall input: Reconstruction of the 8–9 September 2002 catastrophic flood event in the Gard region, France. *Adv. Water Resour.* 32, 1077–1089.
- Borga, M., Anagnostou, E.N., Blöschl, G., Creutin, J.D., 2010. Flash floods: observations and analysis of hydro-meteorological controls. *J. Hydrol.* 394, 1–3.
- Braud, I., Ayrat, P.A., Bouvier, C., Branger, F., Delrieu, G., Coz, J.L., Nord, G., Vandervaere, J.P., Anquetin, S., Adamovic, M., Andrieu, J., Batiot, C., Boudevillain, B., Brunet, P., Carreau, J., Confoland, A., Didon-Lescot, J.F., Domergue, J.M., Douvinet, J., Dramais, G., Freydier, R., Gérard, S., Huza, J., Leblois, E., Bourgeois, O.L., Boursicaud, R.L., Marchand, P., Martin, P., Nottale, L., Patris, N., Renard, B., Seidel, J.L., Taupin, J.D., Vannier, O., Vincendon, B., Wijibrans, A., 2014. Multi-scale hydrometeorological observation and modelling for flash-flood understanding. *Hydrol. Earth Syst. Sci. Discuss.* 11, 1871–1945.
- Burnash, R.J.C., Ferral, R.L., McGuiire, R.A., 1973. A generalized streamflow simulation system; conceptual modeling for digital computers, US Department of Commerce, National Weather Service and State of California Department of Water.
- Burnash, R.J.C., 1995. The NWS river forecasting-catchment modeling. In: Singh, V.J. (Ed.), *Computer Models of Watershed Hydrology*. Water Resources Publication, Highlands Range, Colorado, pp. 311–366.
- Chow, V.T., 1959. *Open-channel Hydraulics*. McGraw-Hill, Book Co., New York, p. 680.
- Cook, A., Merwade, V., 2009. Effect of topographic data, geometric configuration and modeling approach on flood inundation mapping. *J. Hydrol.* 377, 131–142.
- Frey, W.H., 1987. Selective refinement: a new strategy for automatic node placement in graded triangular meshes. *Int. J. Numer. Meth. Eng.* 24 (11), 2183–2200.

- Garambois, P.A., Roux, H., Larnier, K., Labat, D., Dartus, D., 2014. Characterisation of catchment behaviour and rainfall selection for flash flood hydrological models calibration: catchments of the eastern Pyrenees. *Hydrol. Sci. J.* 17, 2305–2322.
- Gesch, B.D., Oimoen, M.J., Evans, G.A., 2014. Accuracy assessment of the U.S. Geological Survey National Elevation Dataset, and comparison with other large-area elevation datasets – SRTM and ASTER, USGS Open-file Report 2014-1008. Available at: <<http://pubs.usgs.gov/of/2014/1008/pdf/ofr2014-1008.pdf>> (accessed September 8, 2014).
- Gourley, J.J., Erlingis, J.M., Hong, Y., Wells, E., 2012. Evaluation of tools used for monitoring and forecasting flash floods in the United States. *Weather Forecasting* 27, 158–173.
- Hardy, R.J., Bates, P.D., Anderson, M.G., 1999. The importance of spatial resolution in hydraulic models for floodplain environments. *J. Hydrol.* 216, 124–136.
- Hong, Y., Hsu, K., Gao, X., Sorooshian, S., 2004. Precipitation estimation from remotely sensed information using an artificial neural network—cloud classification system. *J. Appl. Meteorol.* 43, 1834–1852.
- Horritt, M.S., Bates, P.D., 2002. Evaluation of 1-D and 2-D numerical models for predicting river flood inundation. *J. Hydrol.* 268 (1–4), 87–99.
- Horritt, M.S., Bates, P.D., Mattinson, M.J., 2006. Effects of mesh resolution and topographic representation in 2D finite volume models of shallow water fluvial flow. *J. Hydrol.* 329, 306–314.
- Hsu, K., Gao, X., Sorooshian, S., Gupta, H.V., 1997. Precipitation estimation from remotely sensed information using artificial neural networks. *J. Appl. Meteorol.* 36 (9), 1176–1190.
- Khakbaz, B., Imam, B., Hsu, K., Sorooshian, S., 2012. From lumped to distributed via semi-distributed: calibration strategies for semi-distributed hydrologic models. *J. Hydrol.* 418–419, 61–77.
- Kim, B., Sanders, B.F., Schubert, J.E., Famiglietti, J.S., 2014. Mesh type tradeoffs in 2D hydrodynamic modeling of flooding with a Godunov-based flow solver. *Adv. Water Resour.* 68, 42–61.
- Kim, J., Warnock, A., Ivanov, V.Y., Katopodes, N.D., 2012. Coupled modeling of hydrologic and hydrodynamic processes including overland and channel flow. *Adv. Water Resour.* 37, 104–126.
- Koren, V., Barrett, C.B., 1995. Satellite based, distributed monitoring, forecast, and simulation (MFS) system for the Nile River. In: Kite, G.W., Pietroniro, A., Pultz, T. J. (Eds.), *Application of Remote Sensing in Hydrology*. NHRI, Saskatoon, Canada, pp. 187–200.
- Koren, V., Smith, M., Duan, Q., 2003. Use of a priori parameter estimates in the derivation of spatially consistent parameter sets of rainfall-runoff models. In: Duan, Q., Gupta, H., Sorooshian, S., Rousseau, A., Turcotte, R. (Eds.), *Calibration of Watershed Models: Water Science and Application Series, vol. 6*. American Geophysical Union, Washington, DC.
- Koren, V., Reed, S., Smith, M., Zhang, Z., Seo, D.J., 2004. Hydrology laboratory research modeling system (HL-RMS) of the US National Weather Service. *J. Hydrol.* 291, 297–318.
- Koren, V., Smith, M., Cui, Z., Cosgrove, B., 2007. Physically-based modifications to the sacramento soil moisture accounting model: modeling the effects of frozen ground on the rainfall-runoff process, NOAA Technical Report NWS 52. Available at: <http://www.nws.noaa.gov/oh/hrl/hsmb/docs/hydrology/PBE_SAC-SMA/NOAA_Technical_Report_NWS_52.pdf> (accessed September 8, 2014).
- Liang, X., Lettenmaier, D.P., Wood, E.F., Burges, S.J., 1994. A simple hydrologically based model of land surface water and energy fluxes for GSMs. *J. Geophys. Res.* 99, 415–428.
- McCuen, R., Snyder, W.M., 1975. A proposed index for comparing hydrographs. *Water Resour. Res.* 11 (6), 1021–1024.
- Mersel, M.K., Smith, L.C., Andreadis, K.M., Durand, M.T., 2013. Estimation of river depth from remotely sensed hydraulic relationships. *Water Resour. Res.* 49, 3165–3179.
- National Weather Service (NWS), 2008. Hydrology Laboratory-Research Distributed Hydrologic Model (HL-RDHM) User Manual V. 2.4.2. Available at: <http://www.cbrfc.noaa.gov/present/rdhm/RDHM_User_Manual.pdf> (accessed September 8, 2014).
- Neal, J.C., Schumann, G., Bates, P.D., 2012. A subgrid channel model for simulating river hydraulics and floodplain inundation over large and data sparse areas. *Water Resour. Res.* 48 (11), 16W11506.
- Nguyen, P., Thorstensen, A., Sorooshian, S., Hsu, K., AghaKouchak, A., 2015. Flood forecasting and inundation mapping using HiResFlood-UCI and near-real-time satellite precipitation data: the 2008 Iowa flood. *J. Hydrometeorol.* 16, 1171–1183.
- Rebay, S., 1993. Efficient unstructured mesh generation by means of Delaunay triangulation and Bowyer-Watson algorithm. *J. Comput. Phys.* 106(1), 125–138.
- Reed, S., Koren, V., Smith, M., Zhang, Z., Moreda, F., Seo, D.J., 2004. Overall distributed model intercomparison project results. *J. Hydrol.* 298 (1–4), 27–60.
- Reed, S., Schaake, J., Zhang, Z., 2007. A distributed hydrologic model and threshold frequency-based method for flash flood forecasting at ungauged locations. *J. Hydrol.* 337, 402–420.
- Sanders, B.F., 2007. Evaluation of on-line DEMs for flood inundation modeling. *Adv. Water Resour.* 30, 1821–1843.
- Schumann, G.J.P., Neal, J.C., Voisin, N., Andreadis, K.M., Pappenberger, F., Phanthuwongpakdee, N., Hall, A.C., Bates, P.D., 2013. A first large-scale flood inundation forecasting model. *Water Resour. Res.* 49, 6248–6257.
- Shewchuk, J.R., 1996. Triangle: engineering a 2D quality mesh generator and Delaunay triangulator. *Lect. Notes Comput. Sci.* 1148, 203–222. Available at: <<http://www.cs.berkeley.edu/~jrs/papers/triangle.pdf>> (accessed September 8, 2014).
- Smith, M., Koren, V., Reed, S., Zhang, Z., Zhang, Y., Moreda, F., Cui, Z., Mizukami, N., Anderson, E., Cosgrove, B., 2012a. The distributed model intercomparison project – Phase 2: motivation and design of the Oklahoma experiments. *J. Hydrol.* 418–419, 3–16.
- Smith, M., Koren, V., Zhang, Z., Zhang, Y., Reed, S., Cui, Z., Moreda, F., Cosgrove, B., Mizukami, N., Anderson, E. DMIP 2 Participants, 2012b. Results of the DMIP 2 Oklahoma experiments. *J. Hydrol.* 418–419, 17–48.
- Smith, M., Koren, V., Zhang, Z.Y., Moreda, F., Cui, Z.T., Cosgrove, B., et al., 2013. The distributed model intercomparison project – Phase 2: experiment design and summary results of the western basin experiments. *J. Hydrol.* 507, 300–329.
- Smith, M., Seo, D., Koren, V., Reed, S., Zhang, Z., Duan, Q., Moreda, F., Cong, S., 2004. The distributed model intercomparison project (DMIP): motivation and experiment design. *J. Hydrol.* 298, 4–26.
- Toro, E.F., 2001. *Shock-capturing Methods for Free-surface Shallow Flows*. Wiley, Chichester, U.K., p. 326.